RESEARCH MEMORANDUM

INVESTIGATION OF THE EFFECTS OF BODY INDENTATION AND OF WING-PLAN-FORM MODIFICATION ON THE LONGITUDINAL CHARACTERISTICS OF A 60° SWEPT-WING—BODY COMBINATION AT MACH NUMBERS OF 1.41, 1.61, AND 2.01

By John R. Sevier, Jr.

Langley Aeronautical Laboratory
Langley Field, Va.

CLASSIFIED DOCUMENT

NATIONAL ADVISORY COMMITTEE FOR AERONAUTICS

WASHINGTON

July 25, 1955

NACA RM L55E17

NATIONAL ADVISORY COMMITTEE FOR AERONAUTICS

RESEARCH MEMORANDUM

INVESTIGATION OF THE EFFECTS OF BODY INDENTATION AND OF WING-PLAN-FORM MODIFICATION ON THE LONGITUDINAL CHARACTERISTICS OF A 60° SWEPT-WING—BODY COMBINATION AT MACH NUMBERS OF 1.41, 1.61, AND 2.01

By John R. Sevier, Jr.

SUMMARY

An investigation has been made in the Langley 4- by 4-foot supersonic pressure tunnel to determine the effects of body indentation on the minimum drag and maximum lift-drag ratio of a 60° swept-wing—body combination. A secondary aim of the tests was to determine the effect on the maximum lift-drag ratio of modifying the inboard plan form of the 60° swept wing. The local chords over the inboard portion of the wing were lengthened in order to reduce the thickness ratio (the actual thickness was unchanged) and therefore the wing wave drag. Tests were made at Mach numbers of 1.41, 1.61, and 2.01 and at a Reynolds number of 3.7×10^6 per foot. Lift, drag, and pitching-moment data are presented.

Both the 60° swept wing and the extended-chord wing were tested in combination with three bodies. One body had a parabolic shape (Sears-Haack) and the other two were indented, one for a Mach number of 1.0 and the other for a Mach number of 1.4. The 60° swept wing had an aspect ratio of 4, a taper ratio of 0.33, a maximum camber of approximately 1 percent, and was twisted approximately 5° from root to tip for a uniform load at a lift coefficient of 0.25 for a Mach number of 1.4. Thickness ratio varied from 12 percent at the body center line to 6 percent at the 50 percent semispan station and then remained a constant 6 percent out to the tip.

Results of the 60° swept-wing tests showed that, at a Mach number of 1.41, the indented-body—wing configurations had about 15 to 20 percent higher values of maximum lift-drag ratio as compared with the parabolic-body—wing configuration. At a Mach number of 1.61, the improvement was considerably less (5 to 7 percent); and at a Mach number of 2.01, there was essentially no effect. Similar trends were noted in

minimum drag: at a Mach number of 1.41, there was about a 30-percent decrease in minimum drag for the indented configurations as compared with the parabolic configuration; at a Mach number of 1.61, the decrease was about 18 percent; and at a Mach number of 2.01, the decrease was about 5 percent.

Results of the extended-chord wing tests indicated that, at Mach numbers of 1.61 and 2.01, the maximum lift-drag ratios for the extended-chord configurations were about 15 percent higher than those for the 60° swept-wing configurations. At a Mach number of 1.41, however, there was only a slight improvement. It is of interest to note that the volume of the extended-chord wing was about 40 percent greater than that for the 60° swept wing.

INTRODUCTION

The application of the area rule concept (refs. 1 and 2) to the design of slender-wing—body configurations results in a configuration for which the greatest favorable effects on wave drag occur at the particular design Mach number. In practice, however, an airplane is required to perform efficiently over a range of Mach number. Thus, the aerodynamic characteristics of these area-rule configurations at an off-design Mach number becomes an important question. The purpose of the present report is to evaluate the aerodynamic characteristics (minimum drag coefficient and maximum lift-drag ratio, in particular) for several area rule configurations at their design and off-design Mach numbers.

In reference 2 are reported the results of tests in the Langley 8-foot transonic pressure tunnel of three wing-body combinations in the Mach number range from 0.80 to 1.15. The three bodies consisted of (1) a basic parabolic body (Sears-Haack), (2) a body indented such that the area distribution for the 60° sweptback-wing—body combination at a Mach number of unity was the same as for the basic body alone, and (3) a body indented so as to obtain smooth wing-body area distributions at a Mach number of 1.4. The wing tested in combination with these bodies was swept 60°, cambered and twisted, and was thickened over the inboard 50 percent semispan for improved structural characteristics. Results indicated that, in the transonic range, the indented-body—wing combinations had higher values of maximum lift-drag ratio than the basic parabolic-body—wing combination. It was, therefore, of interest to test these configurations at supersonic speeds, particularly the indented body designed for a Mach number of 1.4, to determine whether similar improvements existed supersonically. Tests have, therefore, been made in the Langley 4- by 4-foot supersonic pressure tunnel of the aforementioned configurations.

In addition to the above-described tests, an attempt was made to increase further the maximum lift-drag ratios (in the supersonic speed range) by means of increasing the wing chord over the thickened portion of the wing and thereby reduce the thickness ratio and the resulting wave drag (ref. 3). The bodies tested with the extended-chord wing were the same as those tested with the original 60° sweptback wing.

The present tests were made at Mach numbers of 1.41, 1.61, and 2.01 and at a Reynolds number of 3.7×10^6 per foot.

SYMBOLS

M	free-stream Mach number
p_o	free-stream stagnation pressure
q	free-stream dynamic pressure
R	Reynolds number
T_o	free-stream stagnation temperature
b	wing span
c	airfoil chord parallel to plane of symmetry
$\bar{c}$	mean aerodynamic chord, $\dfrac{\int_0^{b/2} c^2 dy}{\int_0^{b/2} c\, dy}$
y	spanwise distance measured from plane of symmetry
S	area of basic 60° sweptback wing extended through fuselage to center line, 1 sq ft
S'	area of extended-chord wing extended through fuselage to center line, 1.375 sq ft
α	angle of attack
L	lift force

[redacted]

D	drag force
m	pitching moment about line perpendicular to plane of symmetry and passing through one-quarter-chord position of mean aerodynamic chord
C_L	lift coefficient, L/qS
C_D	drag coefficient, D/qS
C_m	pitching-moment coefficient about one-quarter-chord position of mean aerodynamic chord, $m/qS\bar{c}$
$C_{D_{min}}$	minimum value of drag coefficient
C_{L_α}	lift-curve slope, per radian
L/D	lift-drag ratio
$(L/D)_{max}$	maximum value of lift-drag ratio
$C_{L_{(L/D)_{max}}}$	value of lift coefficient at point of maximum lift-drag ratio
Λ_{LE}	angle of sweep of wing leading edge
Λ_{TE}	angle of sweep of wing trailing edge
λ	wing taper ratio
θ	angle of roll, cutting plane is perpendicular to plane of symmetry at $\theta = 0^\circ$

Primed coefficients refer to the extended-chord wing for which the coefficients are based on the geometry of the extended-chord wing.

TESTS AND APPARATUS

Tunnel

All tests were conducted in the Langley 4- by 4-foot supersonic pressure tunnel which is a rectangular, closed-throat, single-return wind tunnel designed for a Mach number range of 1.2 to 2.2. The test

section Mach number is varied by deflecting horizontal flexible walls against a series of fixed interchangeable templates which have been designed to produce uniform flow in the test section. For the present tests, the test section Mach numbers were 1.41, 1.61, and 2.01; the test-section heights were 4.5, 4.4, and 5.1 feet, respectively; and the tunnel width was 4.5 feet.

Models

A total of six wing-body configurations were tested in the present investigation: three bodies were tested in combination with a 60° swept-back wing (fig. 1) and the same three bodies were tested in combination with the extended-chord wing (fig. 2).

Wings.- The basic wing used for the investigation had an aspect ratio of 4.0, a taper ratio of 0.33, and was swept 60° at the one-quarter chord. Thickness ratio varied from 12 percent at the model center line to 6 percent at the 50 percent semispan station and then remained a constant 6 percent out to the tip (fig. 3). An NACA 64A series airfoil section in the free-stream direction was used. In order to obtain further favorable effects on lift-drag ratio, the wing was cambered and twisted (fig. 3). The basis for the camber and twist used is the mean surface form theoretically required for a uniform loading at a lift coefficient of 0.25 at a Mach number of 1.4 (ref. 4). This theoretical form has been modified somewhat by reducing the twist near the wind-body juncture.

For the extended-chord wing-body tests, the wing plan form over the inboard 50 percent semispan was modified by extending the local chords forward and rearward, the absolute thickness being left unchanged, such that the resulting wing had a constant-thickness ratio of 6 percent. At the model center line, the basic chord was increased by one-third in the forward direction and by two-thirds in the rearward direction; this increase in the local chord then decreased linearly to zero at the 50 percent semispan station (fig. 2). The aspect ratio for the extended-chord wing was 2.91. Because of an error in design, the extended-chord wing failed to preserve the same twist distribution (over the inboard portion) as the 60° sweptback wing. Instead of having approximately 0° incidence at the wing-body juncture as did the 60° wing, the extended-chord wing had about -3° incidence at this point. From this point outboard the difference in twist between the two wings decreased until, at the 50 percent semispan station, the two wings were identical. The effect of this different twist distribution on the characteristics of the extended-chord wing and on the comparison between the two wings is unknown.

Bodies.- The bodies tested (always in combination with a wing) consisted of the following: (1) a basic parabolic body (Sears - Haack),

(2) a body indented for a Mach number of 1.0 such that the distribution of cross-sectional area for this body in combination with the 60° wing was the same as for the basic parabolic body alone, and (3) a body indented so as to obtain smooth area distributions at a Mach number of 1.4 for the body in combination with the 60° sweptback wing. For this latter body, the indentation was obtained by using a weighted average of the area distributions at roll angles of 0°, 45°, and 90°. A more detailed discussion of the derivation of these bodies can be found in reference 2. Body coordinates are given in table I.

Area distributions for the various bodies in combination with the 60° sweptback wing are presented in figures 4 to 6, whereas area distributions for the extended-chord wing-body configurations are shown in figures 7 and 8.

TESTS

The three bodies previously described were tested in combination with both the 60° sweptback wing and the extended-chord wing through an angle-of-attack range of approximately -4° to 12°.

The test conditions were as follows:

Mach number	p_o, lb/sq in. absolute	T_o, °F	R per foot
1.41	12.38	100°	3.70×10^6
1.61	12.94	100°	3.70×10^6
2.01	14.98	100°	3.70×10^6

Lift, drag, and pitching-moment data were measured by means of a three-component internal strain-gage balance housed within the model. Corrections were applied to all data such that the base pressure was adjusted to free-stream static pressure.

Angle of attack was corrected for deflection due to air loads by using static-deflection data. This method has been checked optically and was found to be accurate to ±0.05°.

PRESENTATION OF RESULTS

In figures 9 to 12 are presented the basic data for the 60° swept-wing—body combination at the three test Mach numbers. Curves of L/D, C_D, and C_L are plotted as a function of angle of attack, and C_m is plotted as a function of C_L.

Data for the extended-chord wing-body combinations are presented in figures 13 to 16 in a manner parallel to the basic 60° wing presentation just described. It should be noted that the coefficients presented for the extended-chord wing configurations are based on the area of the extended-chord wing. Any comparison of the two wings on an actual force basis would be misleading.

For a comparison between the 60° sweptback wing and the extended-chord wing, a plot of L/D against C_L for all configurations tested is shown in figure 17. Also shown for comparison purposes is a plot of C_m against C_L for the $M = 1.4$ body in combination with the 60° swept wing and with the extended-chord wing (fig. 18). In both figures the coefficients are based on the geometry of the particular wing under consideration.

Summary plots of the more important results are shown in figures 19 to 23. Certain transonic data (ref. 2) are also shown in these figures for the sake of completeness.

For general comparison purposes, results of a similar configuration tested at the Ames Aeronautical Laboratory (ref. 5) are included in figure 22. The wing of reference 5 was swept 60.8° at the quarter chord, had an aspect ratio of 3.5, a taper ratio of 0.25, had NACA 64A sections cambered and twisted, and had a thickness ratio of 5 percent. Thus, the wing is comparable with the 60° swept wing of the present report with the exception of thickness ratio. The body tested in reference 5 was very similar to the basic parabolic body of the present report. Thus, the comparison of the two wings in combination with the parabolic bodies (fig. 22) reflects the effect of thickness ratio and shows, as would be expected in the supersonic range, that the wing-body of reference 5 has an appreciably higher value of $(L/D)_{max}$ than the present wing-body.

RESULTS AND DISCUSSION

60° swept-wing—body configurations.- In reference 2 are reported the results of tests made in the Langley 8-foot transonic pressure tunnel of the 60° swept-wing—body configurations considered herein. Three

bodies were tested: one was a parabolic reference body and the other two were indented, one for a Mach number of unity (transonic area rule) and one for a Mach number of 1.4 (supersonic area rule). The Mach number range of these tests was 0.80 to 1.15. Results of these tests indicated that the minimum drag of these wing-body combinations could be reduced significantly in the transonic range by means of body indentation. At the highest test Mach number of 1.15, there was about a 35-percent reduction in $C_{D_{min}}$ for both the indented bodies as compared with the parabolic reference body (fig. 19). In the supersonic speed range investigated in the present report, similar improvements were noted but became less at the higher (off-design) Mach numbers, as might be expected. At a Mach number of 1.41, the minimum drag coefficient of both the indented-body configurations was about 30 percent less than that for the parabolic-body-wing-configuration, the $M = 1.4$ configuration being slightly better than the $M = 1.0$ configuration. At a Mach number of 1.61, the corresponding improvement was 18 percent; at $M = 2.01$, there was only about 5-percent reduction.

It is of interest to note the small difference in minimum drag between the two indented configurations throughout the Mach number range. This result is consistent with the fact that the area distributions of the two configurations are very similar throughout the speed range. At a Mach number of 1.4, for example, there is a difference of only 0.001 in $C_{D_{min}}$ even though one of the configurations is at its design Mach number and the other configuration is considerably off the design Mach number. Examination of figures 5 and 6 shows that this is to be expected because of the similarity of the area distribution at $M = 1.4$. At a Mach number of 1.61, a visual inspection of the area diagrams shows that the area distributions of both indented configurations are poor; thus, the reduction in $C_{D_{min}}$ would not be expected to be as great as that at $M = 1.41$. Similar reasoning applies at $M = 2.01$ where the area distributions (not shown) would be even worse than those at the lower Mach numbers. In order to get a quantitative result from the area diagrams, it would be necessary actually to compute the wave drag of the configurations by using the method of Holdaway (ref. 6).

Variation of lift-curve slope with Mach number is shown in figure 20. Inspection of these data indicates that body indentation has very little effect on lift characteristics.

Figure 21 shows the variation of $(L/D)_{max}$ with Mach number and includes the Mach number range of reference 2. At a Mach number of 1.15, the results of reference 2 indicate about a 50-percent increase in $(L/D)_{max}$ for both the indented bodies as compared with the parabolic body. From the present tests, results indicate that at $M = 1.41$ this improvement decreased to about 20 percent for the $M = 1.4$ body-wing configuration

[redacted]

and about 15 percent for the $M = 1.0$ configuration. The maximum lift-drag ratio $(L/D)_{max}$ for the parabolic body was 7.32. At a Mach number of 1.61, the corresponding improvements for the two bodies were 7 percent and 5 percent over the parabolic-body value of 6.46. At a Mach number of 2.01, there is essentially no effect due to indentation (fig. 21). Thus, this investigation has shown that for the particular configurations tested, superior performance $\left(C_{D_{min}}\right.$ and $\left.(L/D)_{max}\right)$ in the transonic range can be made to extend into the supersonic range, the effects of indentation, at worst, never becoming very detrimental (up to $M = 2.01$).

A further advantage of the indented-body—wing configurations is in the reduction of the lift coefficient at which maximum lift-drag ratio occurs (fig. 23). At a Mach number of 1.41, $(L/D)_{max}$ occurs at a lift coefficient of 0.26 for the basic body; whereas, for the $M = 1.4$ indented body, the optimum lift coefficient is 0.20, a reduction of about 23 percent. A similar comparison at the higher Mach numbers indicates a 16-percent reduction at $M = 1.61$, none at $M = 2.01$.

In order not to preclude the possibility of further drag reduction and better characteristics over the Mach number range, other methods of fuselage modification such as those described in references 7 and 8 are brought to the attention of the reader.

Extended-chord wing.- The basic idea behind the extended-chord scheme is chiefly to achieve a reduction in wave drag by means of decreasing the thickness ratio without changing the actual thickness (ref. 3). Thus, the thickness necessary for proper structural characteristics can be achieved wihhout paying the wave-drag penalty for high thickness ratio. Associated with the decreased wave drag is an increase in skin-friction drag due to the increased chord, although this latter effect is generally small. At the same time substantial increases in wing volume (important from stowage considerations) are realized. For the present configuration, the exposed-wing volume was increased by about 40 percent over the volume of the original 60° sweptback wing. This increase in volume becomes an especially important consideration when it is noted that the improved characteristics of the indented-body configurations are attained at the expense of reduced fuselage volume.

It is to be emphasized that no attempt was made to evaluate the effectiveness of various extended-chord configurations as was done in reference 3. The results of reference 3 indicated that, for a given amount of chord extension, best results were obtained with one-third of it forward and two-thirds rearward. With this consideration in mind, the present extended-chord wing was designed so as to modify the original 60° sweptback wing to one of constant 6-percent-thickness ratio. In testing the same three bodies with the extended-chord wing as were designed to be

tested with the 60° swept wing, it is obvious that no effort was made to maintain smooth area distributions for the indented-body—wing configurations (figs. 7 and 8).

Results of the present tests indicate that, for the particular configurations considered herein, at Mach numbers of 1.61 and 2.01, about a 15-percent increase in maximum lift-drag ratio can be obtained through the use of the extended-chord wing. For example, at a Mach number of 1.61, the original 60° swept wing in combination with the $M = 1.4$ body has an $(L/D)_{max}$ of 6.93; the corresponding value for the same body with the extended-chord wing is 7.91 (fig. 21). At a Mach number of 1.41, however, the extended-chord scheme resulted in only a slight improvement in $(L/D)_{max}$ (5 percent) for the parabolic-body—wing and the $M = 1.0$ body-wing configurations, and no improvement for the $M = 1.4$ body-wing configuration.

Figure 19 shows the variation of minimum drag coefficient for the extended-chord configurations (together with the 60° sweptback-wing—body configurations). The drag coefficients for the extended-chord configurations are based on the area of the extended-chord wing and are therefore not valid for comparing actual drag forces between the two wings (fig. 19(a)). For this reason, figure 19(b) in which the drag coefficients of the extended-chord configurations are based on the area of the 60° sweptback wing is included. This latter figure is then indicative of actual drag force characteristics. Examination of figure 19 shows that, at a Mach number of 2.01, although the drag coefficient for the extended-chord wing-body comfiguration is about 30 percent less than that for the 60° swept-wing—body configuration, the actual drag force is about the same. At a Mach number of 1.61, the drag coefficient is about 23 percent lower whereas the drag force is again about the same. At a Mach number of 1.41, the minimum drag force for the extended-chord configurations is higher than that for the 60° swept-wing configurations.

A visual analysis of the area distributions (figs. 5 to 8) shows that this trend of minimum drag is not inconsistent with the predictions of the area rule, at least at $M = 1.41$. At this Mach number the area distributions of the 60° swept-wing configurations are smoother than those for the extended-chord configurations; consequently, the wave drag is expected to be lower. At $M = 1.61$, the area distributions of both configurations are rather irregular; thus, a more detailed analysis would be required (ref. 6).

Lift-curve-slope variation with Mach number is shown in figure 20. The slope was measured over an angle-of-attack range of approximately 0° to 6°. The same caution about comparison applies here as in the case of drag coefficient; figure 20(b) is indicative of actual lift force and shows that, at a given angle of attack, the extended-chord wing has greater lift. Therefore, in order to sustain a given lift, the extended-chord wing-body configuration requires a lower angle of attack than the

60° swept-wing—body configuration. Such a result indicates that a comparison of the drag forces of the two wing configurations at some flight lift coefficient rather than that for minimum drag would show the extended-chord wing in a more favorable light. For example, consider the most unfavorable case for minimum drag comparison, that of the $M = 1.4$ body-wing configurations at $M = 1.41$. From figure 19 it can be seen that the minimum drag force of the extended-chord configuration is about 35 percent more than that for the 60° swept-wing configuration. If a comparison is made of the drag forces of the two configurations at some flight lift coefficient, say $C_L = 0.25$, it will be seen that, for the 60° wing, $M = 1.4$ body configuration, the corresponding drag coefficient is 0.03; whereas in order to maintain the same lift force for the extended-chord configuration, a lift coefficient of only 0.18 is required with a corresponding drag coefficient (based on the 60° wing area) of 0.029. Thus, for this simplified case, the extended-chord wing actually shows a slight reduction in drag force at $C_L = 0.25$.

Examination of figure 18, which shows pitching-moment data for the $M = 1.4$ body-wing configurations, illustrates an interesting aspect of the extended-chord wing. At a Mach number of 1.41 and, to some extent, at $M = 1.61$, the 60° swept-wing—body configurations had a pitch-up tendency near a lift coefficient of 0.2. This effect was found in the transonic tests (ref. 9) and was even more pronounced near a lift coefficient of 0.6. Figure 18 shows this condition to be relieved greatly for the extended-chord wing and $M = 1.4$ body configuration. Similar results were obtained for the $M = 1.0$ body in combination with the extended-chord wing. Balance limits prevented testing at the higher pitch-up lift coefficient; consequently, the effect of the extended-chord wing in relieving pitch-up at supersonic speeds is not completely known. In addition, the effect at transonic speeds has not been investigated.

CONCLUSIONS

An investigation has been made in the Langley 4- by 4-foot supersonic pressure tunnel of the effects of body indentation and of inboard wing-plan-form modification on the longitudinal characteristics of 60° swept-wing—body combinations at Mach numbers of 1.41, 1.61, and 2.01. The results indicate the following conclusions:

(1) For the particular configurations considered herein, at a Mach number of 1.41 (where the greatest improvements were obtained), a comparison of the indented-body—wing configurations with the parabolic-body—wing configuration indicates that body indentation lowered the minimum drag coefficient up to a maximum of 30 percent and increased the maximum lift-drag ratio up to a maximum of 20 percent.

[redacted]

(2) The magnitude of the improvements due to body indentation decreases rapidly with Mach number. At a Mach number of 1.41, the 15- to 20-percent increase in maximum lift-drag ratio for the indented-body configurations is less than half that obtained at a Mach number of 1.15 from previous tests. Above a Mach number of 1.41, where the area distributions become poor (off-design Mach numbers), the improvement in maximum lift-drag ratios for the indented configurations rapidly becomes insignificant.

(3) There was very little difference in maximum lift-drag ratio or minimum drag coefficient between the configuration designed for a Mach number of 1.0 and the one designed for a Mach number of 1.4 because of the similarity in area distributions of these two configurations.

(4) For the extended-chord wing-body configurations tested, increases in maximum lift-drag ratios of about 15 percent were obtained at Mach numbers of 1.61 and 2.01 along with about 40-percent increase in wing volume. At a Mach number of 1.41, however, there was only a slight improvement in maximum lift-drag ratio over the 60° swept-wing—body configurations.

(5) Increasing the local chords over the inboard portion of the wing was useful in relieving the pitch-up tendency near a lift coefficient of 0.2 exhibited by the original 60° swept wing at the test Mach numbers.

Langley Aeronautical Laboratory,
National Advisory Committee for Aeronautics,
Langley Field, Va., April 29, 1955.

[redacted]

REFERENCES

1. Whitcomb, Richard T.: A Study of the Zero-Lift Drag-Rise Characteristics of Wing-Body Combinations Near the Speed of Sound. NACA RM L52H08, 1952.

2. Whitcomb, Richard T., and Fischetti, Thomas L.: Development of a Supersonic Area Rule and an Application to the Design of a Wing-Body Combination Having High Lift-to-Drag Ratios. NACA RM L53H31a, 1953.

3. Cooper, Morton, and Sevier, John R., Jr.: Effects of a Series of Inboard Plan-Form Modifications on the Longitudinal Characteristics of Two 47° Sweptback Wings of Aspect Ratio 3.5, Taper Ratio 0.2, and Different Thickness Distributions at Mach numbers of 1.61 and 2.01. NACA RM L53E07a, 1953.

4. Jones, Robert T.: Estimated Lift-Drag Ratios at Supersonic Speed. NACA TN 1350, 1947.

5. Hall, Charles F., and Heitmeyer, John C.: Aerodynamic Study of a Wing-Fuselage Combination Employing a Wing Swept Back 63° - Characteristics at Supersonic Speeds of a Model With the Wing Twisted and Cambered for Uniform Load. NACA RM A9J24, 1950.

6. Holdaway, George H.: Comparison of Theoretical and Experimental Zero-Lift Drag-Rise Characteristics of Wing-Body-Tail Combinations Near the Speed of Sound. NACA RM A53H17, 1953.

7. Jones, Robert T.: Theory of Wing-Body Drag at Supersonic Speeds. NACA RM A53H18a, 1953.

8. Howell, Robert R., and Braslow, Albert L.: An Experimental Study of a Method of Designing the Sweptback-Wing—Fuselage Juncture for Reducing the Drag at Transonic Speeds. NACA RM L54L31a, 1955.

9. Fischetti, Thomas L.: Effects of Fences, Leading-Edge Chord-Extensions, Boundary-Layer Ramps, and Trailing-Edge Flaps on the Longitudinal Stability of a Twisted and Cambered 60° Sweptback-Wing—Indented-Body Configuration at Transonic Speeds. NACA RM L54D09a, 1954.

[redacted]

TABLE I

BODY COORDINATES

(a) Forebody

Fuselage station, in. from nose	Radius, in.
0	0
.5	.165
1.0	.282
1.5	.378
2.0	.460
2.5	.540
3.0	.612
3.5	.680
4.0	.743
4.5	.806
5.0	.862
5.5	.917
6.0	.969
6.5	1.015
7.0	1.062
7.5	1.106
8.0	1.150
8.5	1.187
9.0	1.222
9.5	1.257
10.0	1.290
10.5	1.320
11.0	1.350
11.5	1.380
12.0	1.405
12.5	1.430
13.0	1.452
13.5	1.475

(b) Afterbody

Fuselage station, in. from nose	Radius, in.		
	Basic body	M = 1.4 body	M = 1.0 body
14.0	1.493	1.461	1.470
14.5	1.512	1.440	1.460
15.0	1.526	1.410	1.440
15.5	1.540	1.365	1.400
16.0	1.552	1.318	1.360
16.5	1.565	1.270	1.320
17.0	1.575	1.226	1.260
17.5	1.585	1.195	1.220
18.0	1.590	1.170	1.190
18.5	1.598	1.150	1.170
19.0	1.602	1.140	1.150
19.5	1.606	1.140	1.140
20.0	1.606	1.160	1.140
20.5	1.604	1.200	1.160
21.0	1.602	1.250	1.200
21.5	1.600	1.280	1.250
22.5	1.587	1.310	1.299
23.5	1.570	1.335	1.328
24.0	1.560	1.345	1.340
25.0	1.532	1.350	1.350
26.0	1.501	1.350	1.350
27.0	1.460	1.330	1.330
28.0	1.414	1.310	1.310
29.0	1.364	1.271	1.280
30.0	1.305	1.230	1.230
31.0	1.231	1.180	1.180
31.7	1.185	1.150	1.150

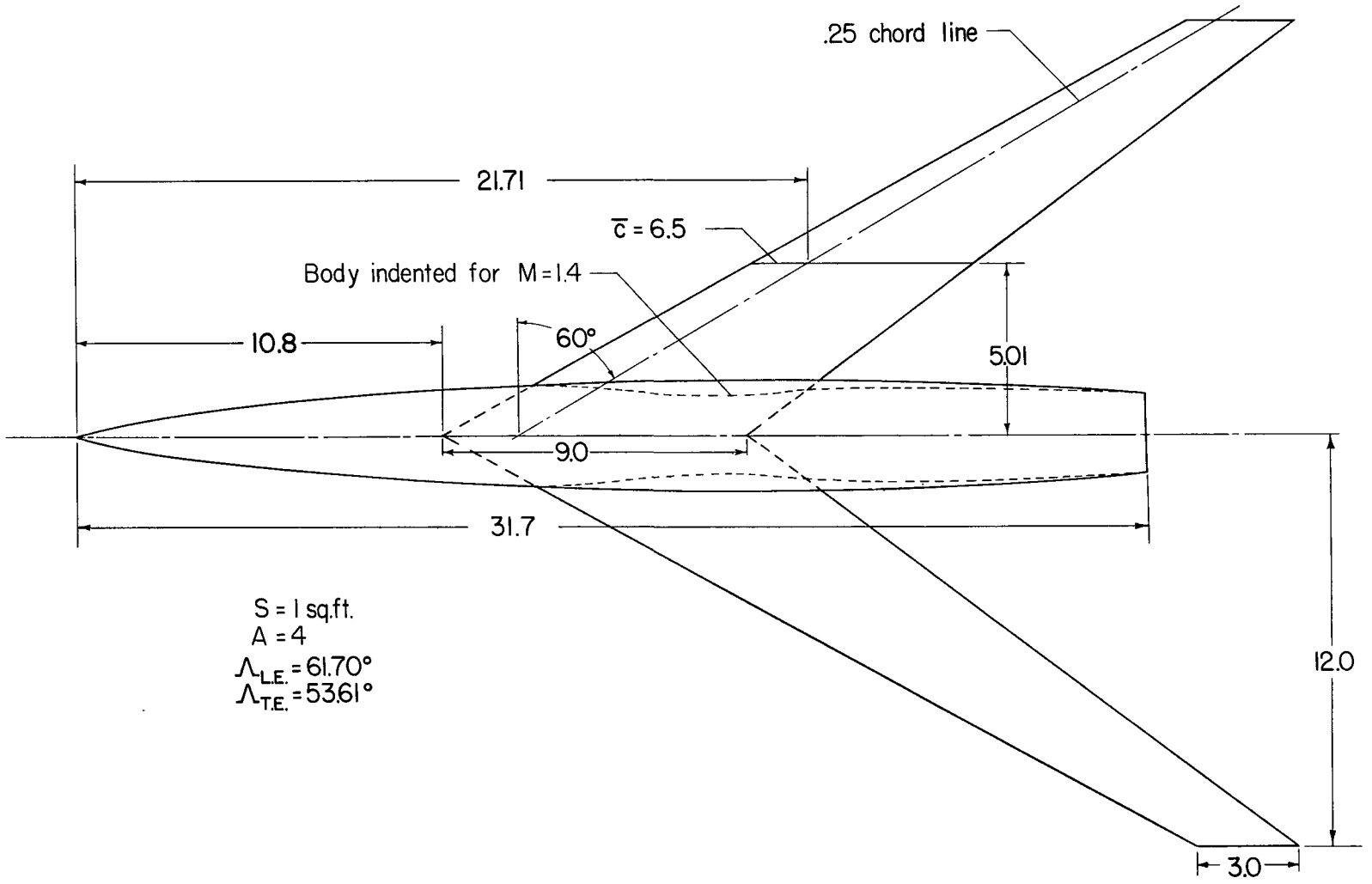

Figure 1.- General arrangement of the 60° swept-wing—body configuration.
All dimensions are in inches.

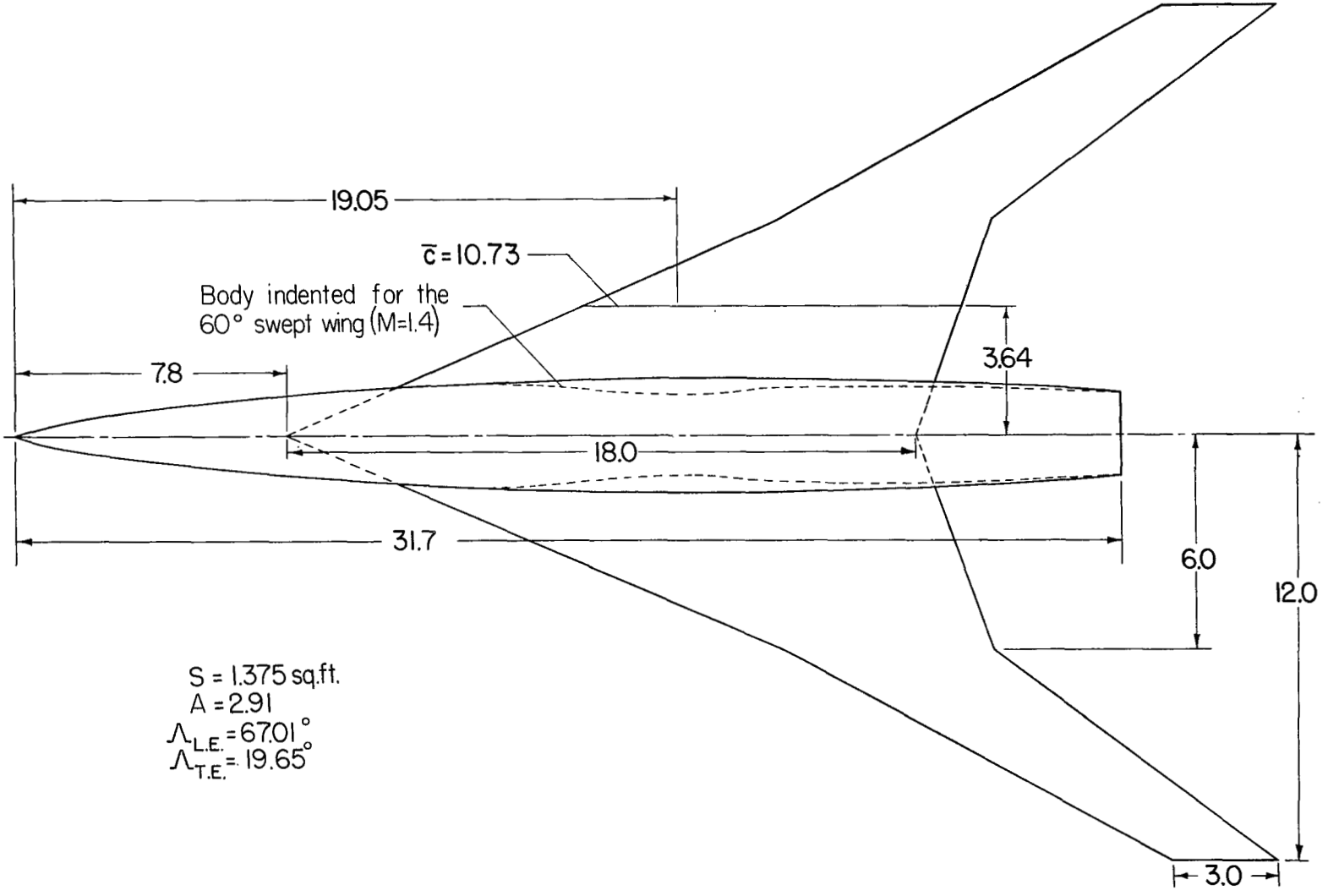

Figure 2.- General arrangement of the extended-chord wing-body configuration. All dimensions are in inches.

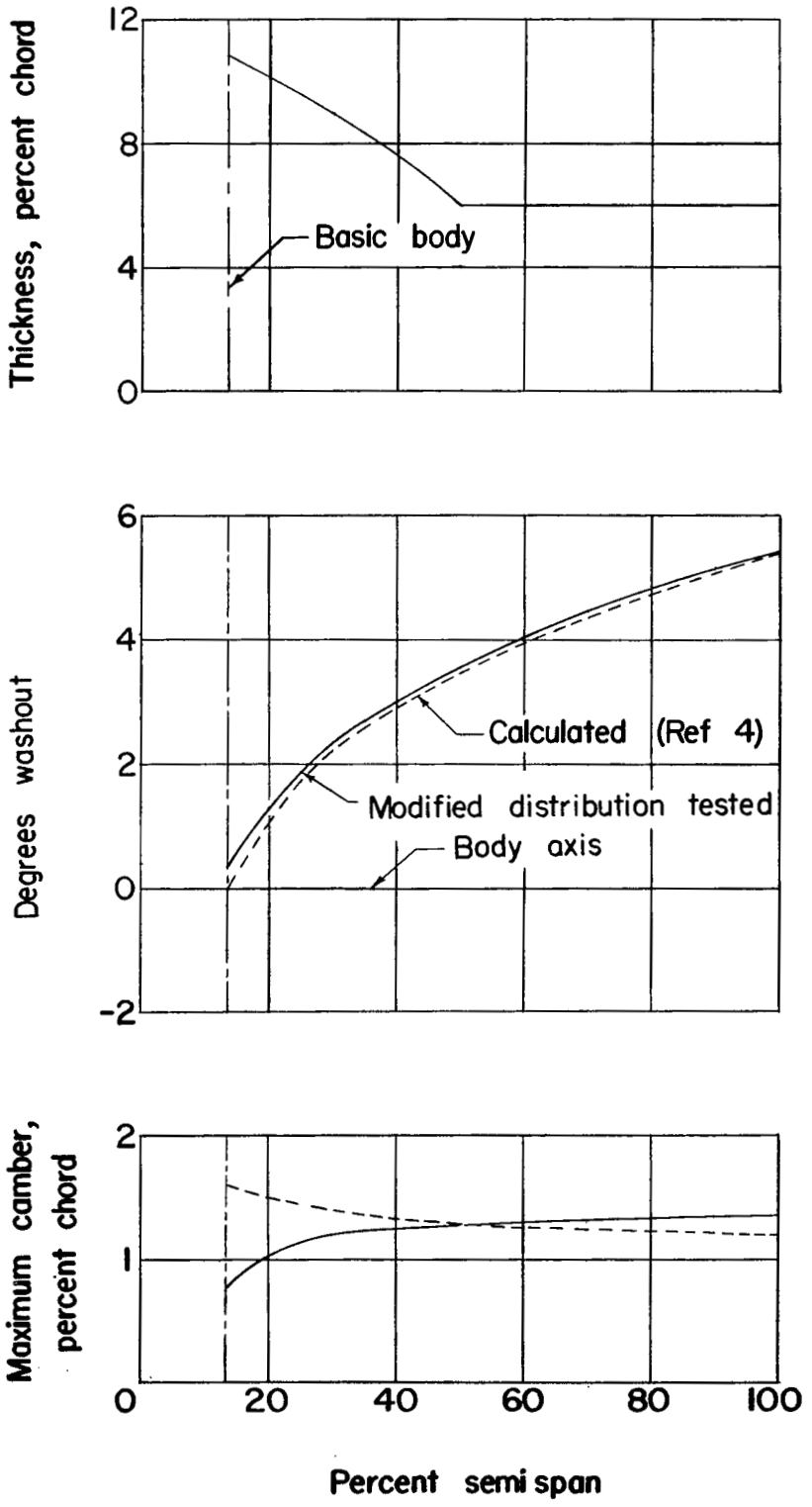

Figure 3.- Spanwise variation of thickness ratio, camber, and twist the 60° swept wing.

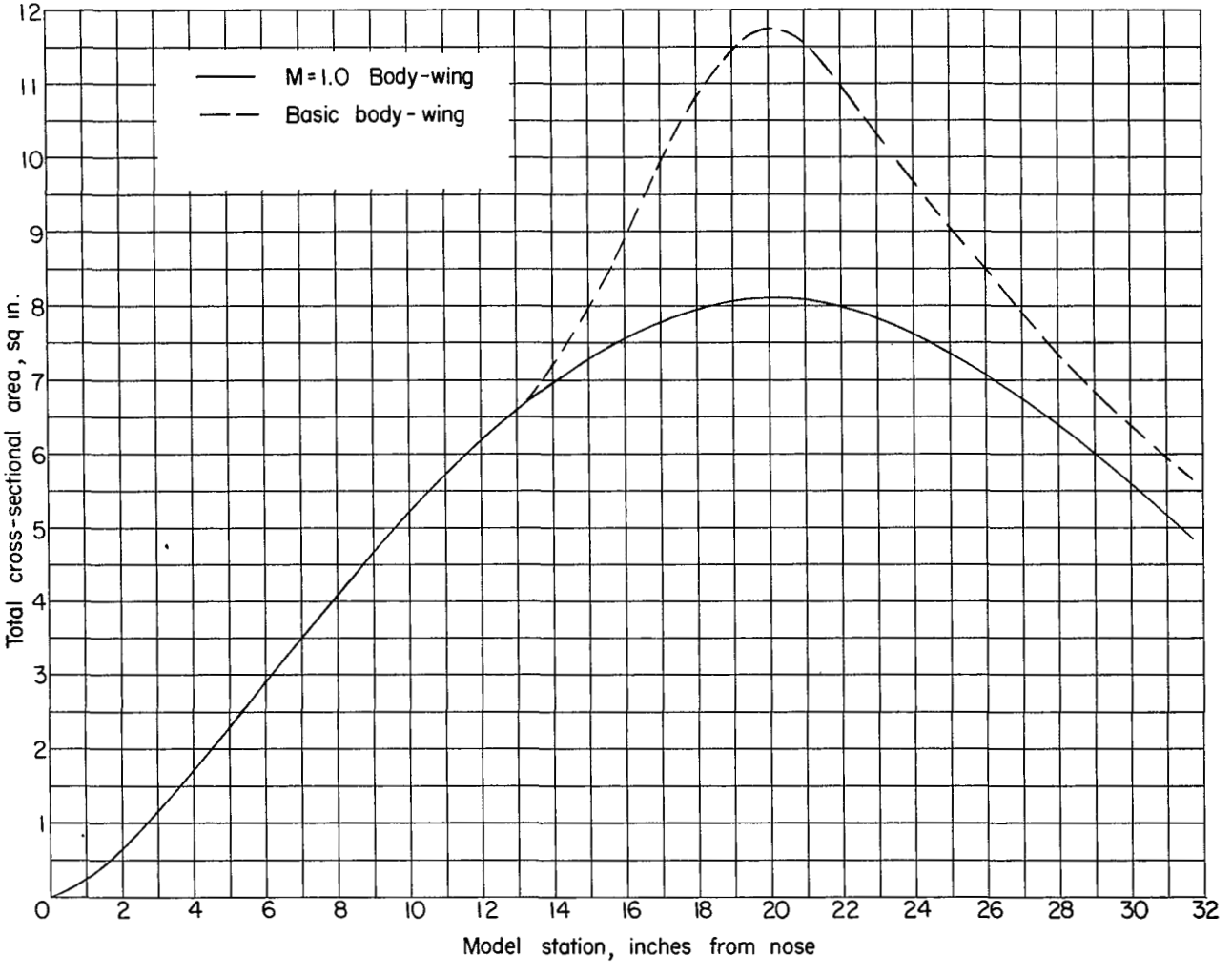

Figure 4.- Axial distribution of cross-sectional area for 60° swept wing in combination with the basic body and a body indented for Mach number of 1.0 at a Mach number of 1.0.

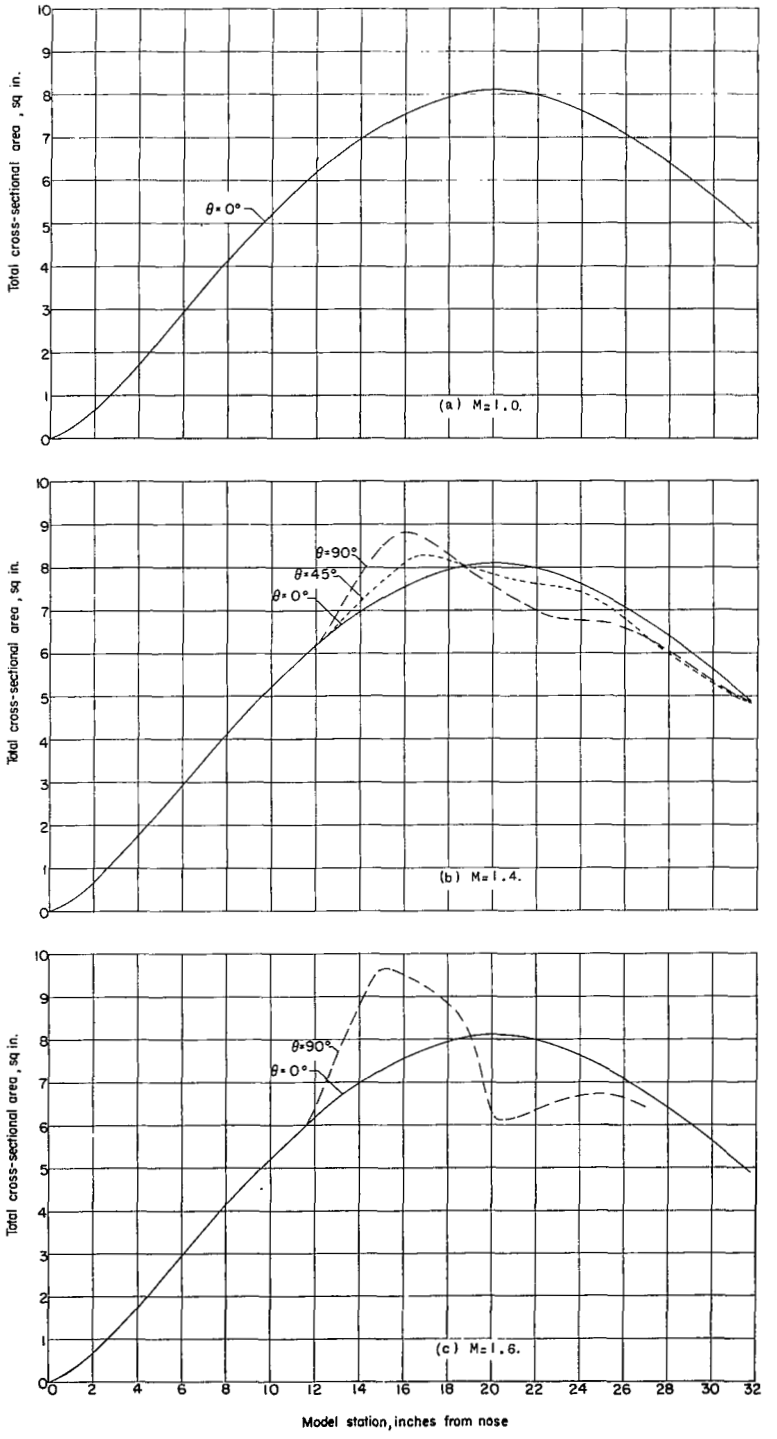

Figure 5.- Axial distribution of cross-sectional area for the 60° swept wing in combination with the body indented for a Mach number of 1.0 at Mach numbers of 1.0, 1.4, and 1.6.

[redacted]

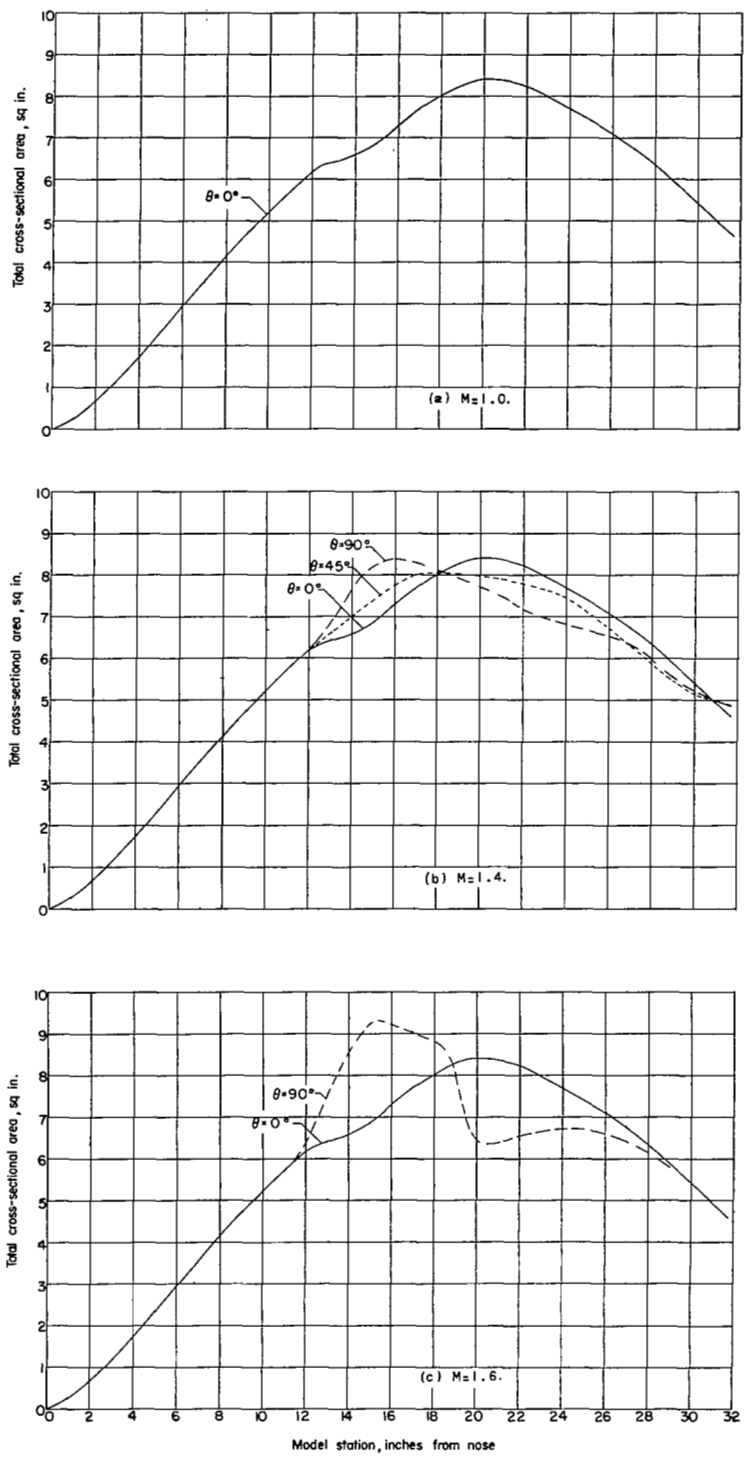

Figure 6.- Axial distribution of cross-sectional area for the 60° swept wing in combination with the body indented for a Mach number of 1.4 at Mach numbers of 1.0, 1.4, and 1.6.

[redacted]

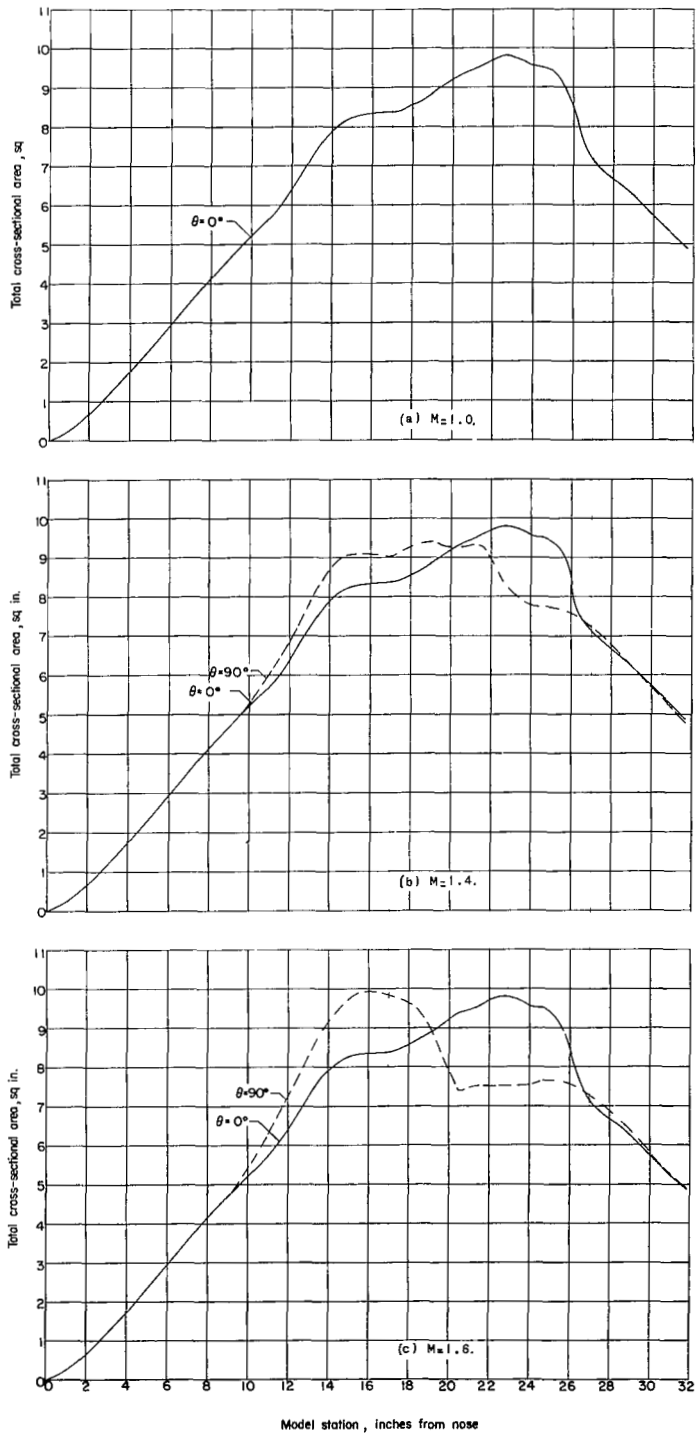

Figure 7.- Axial distribution of cross-sectional area for the extended-chord wing in combination with the body indented for a Mach number of 1.0 at Mach numbers of 1.0, 1.4, and 1.6.

[redacted]

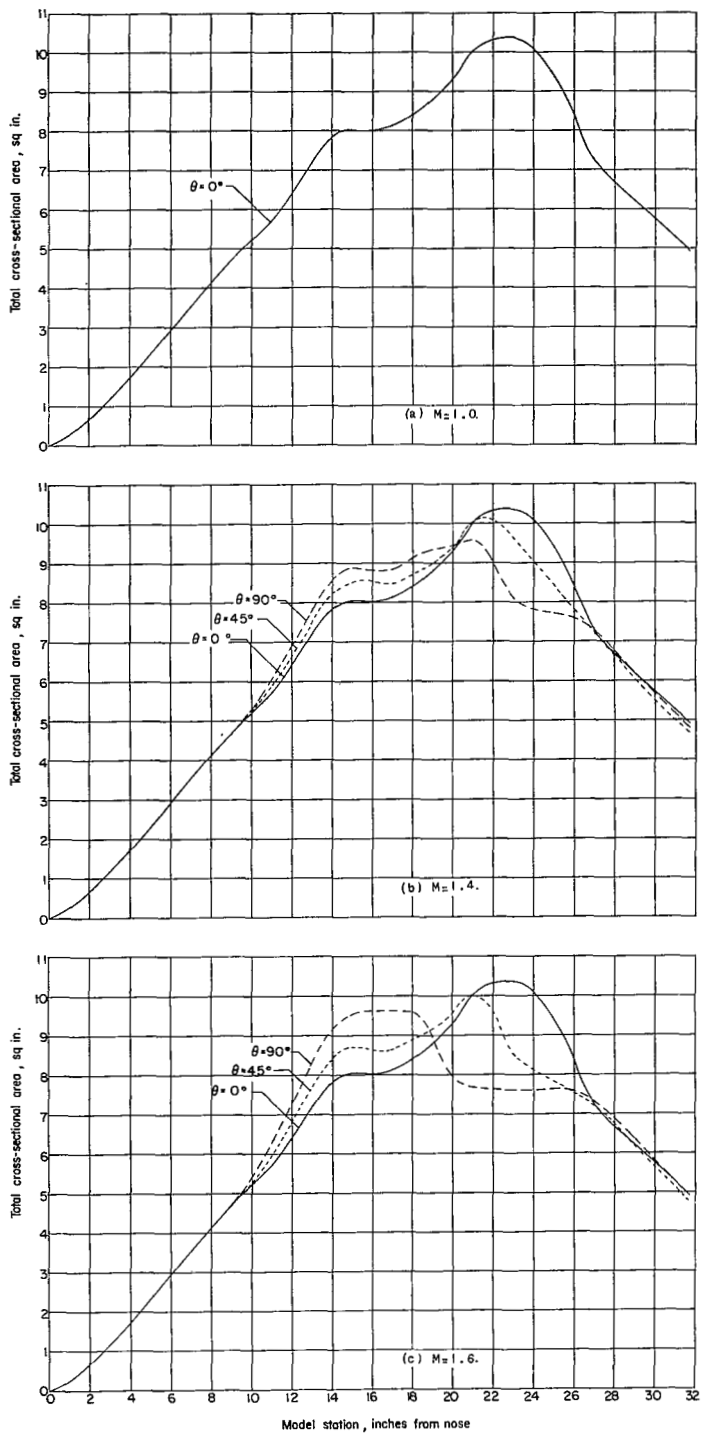

Figure 8.- Axial distribution of cross-sectional area for the extended-chord wing in combination with the body indented for a Mach number of 1.4 at Mach numbers of 1.0, 1.4, and 1.6.

[redacted]

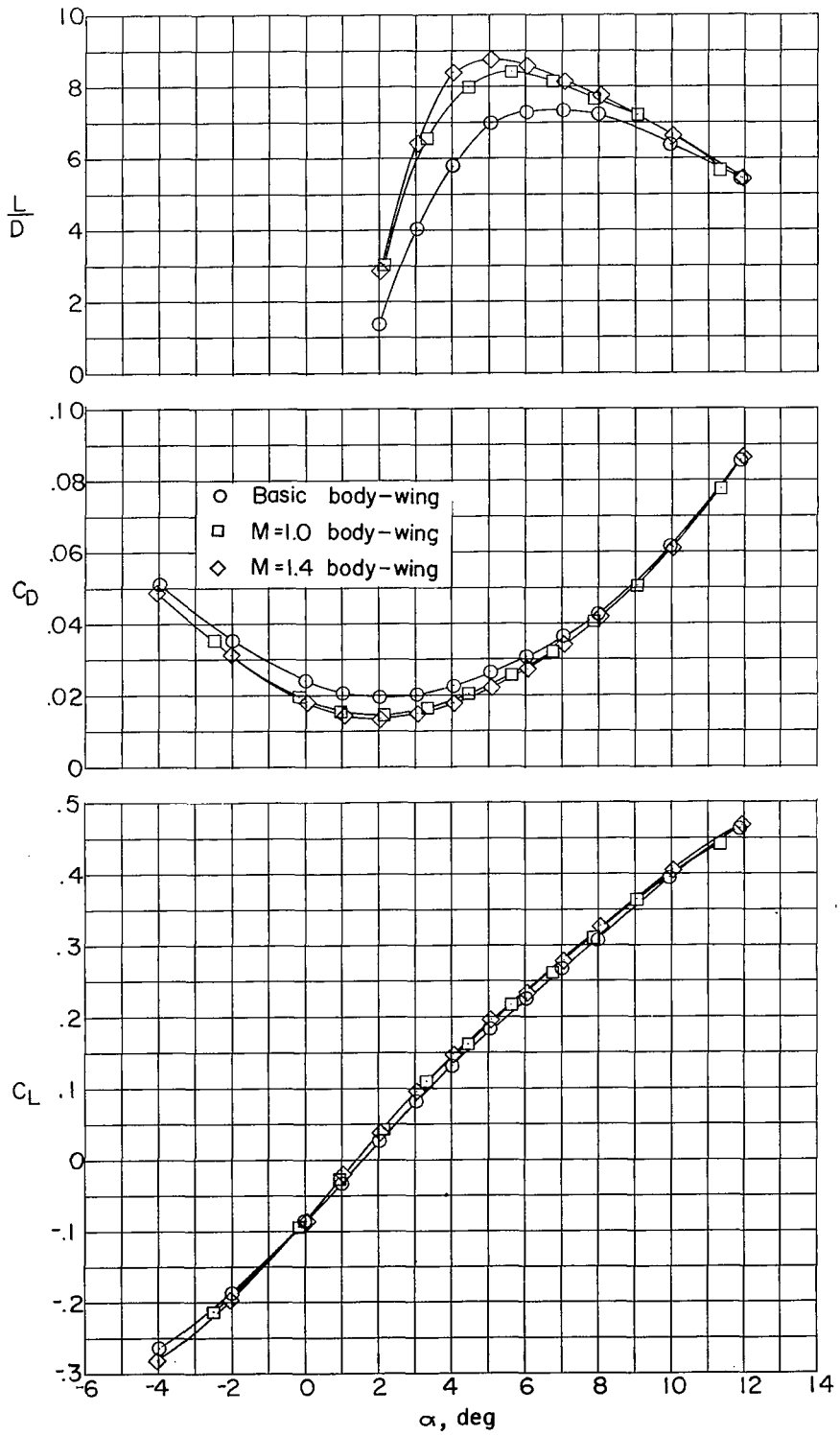

Figure 9.- Lift and drag characteristics of the three bodies in combination with the 60° swept wing at a Mach number of 1.41.

[redacted]

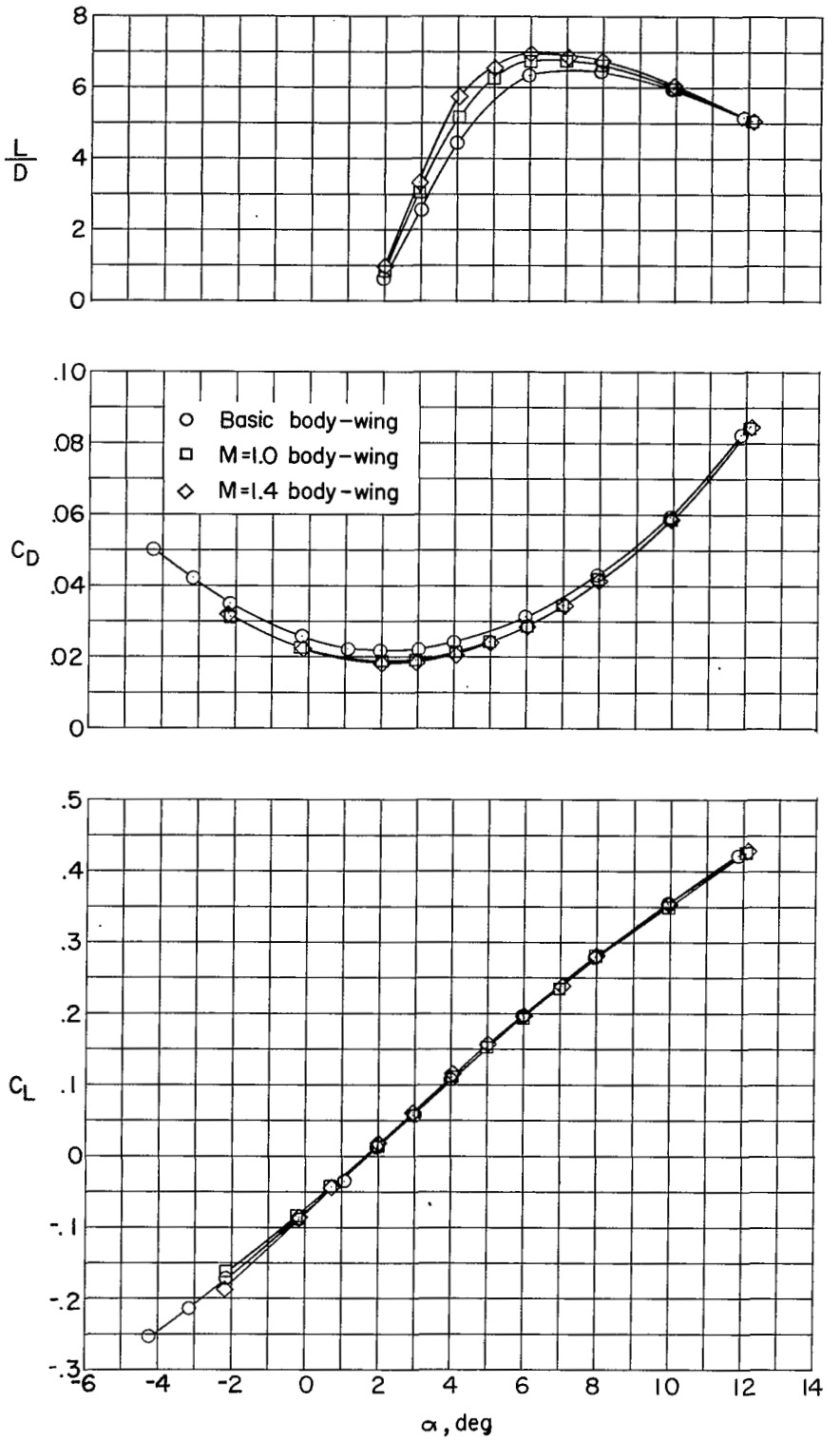

Figure 10.- Lift and drag characteristics of the three bodies in combination with the 60° swept wing at a Mach number of 1.61.

[redacted]

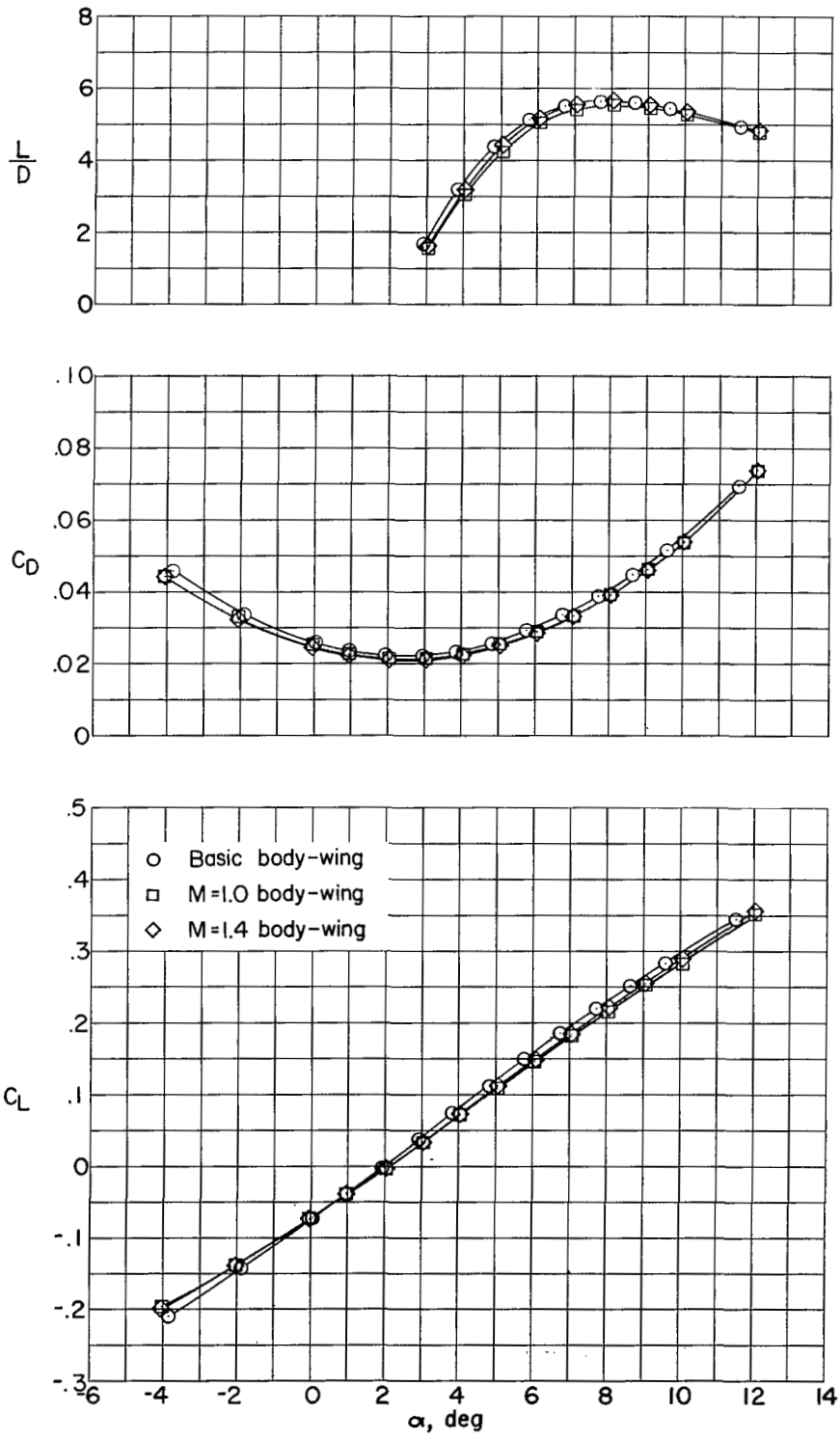

Figure 11.- Lift and drag characteristics of the three bodies in combination with the 60° swept wing at a Mach number of 2.01.

[redacted]

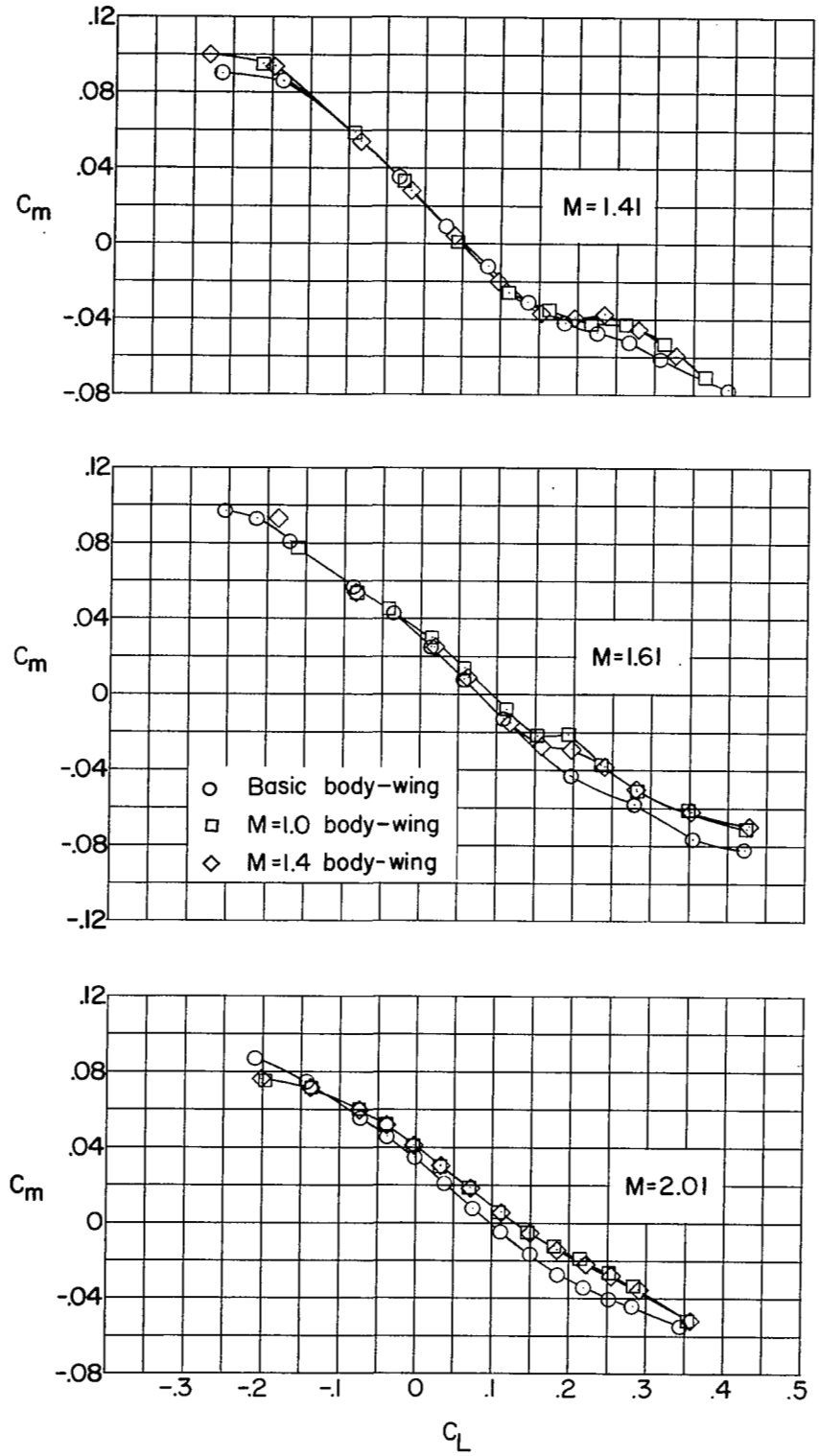

Figure 12.- Pitching-moment characteristics of the three bodies in combination with the 60° swept wing at Mach numbers of 1.41, 1.61, and 2.01.

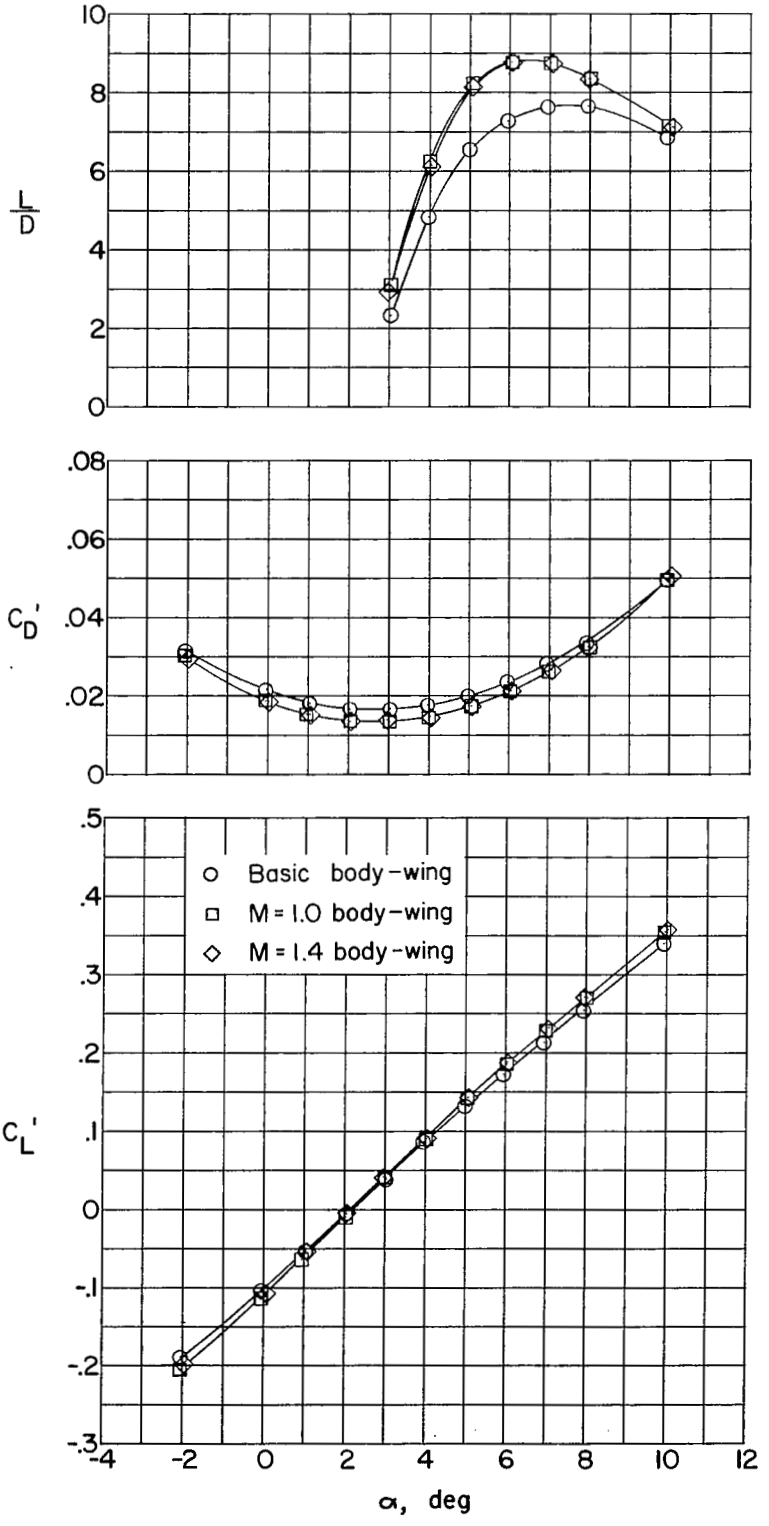

Figure 13.- Lift and drag characteristics of the three bodies in combination with the extended-chord wing at Mach numbers of 1.41.

[redacted]

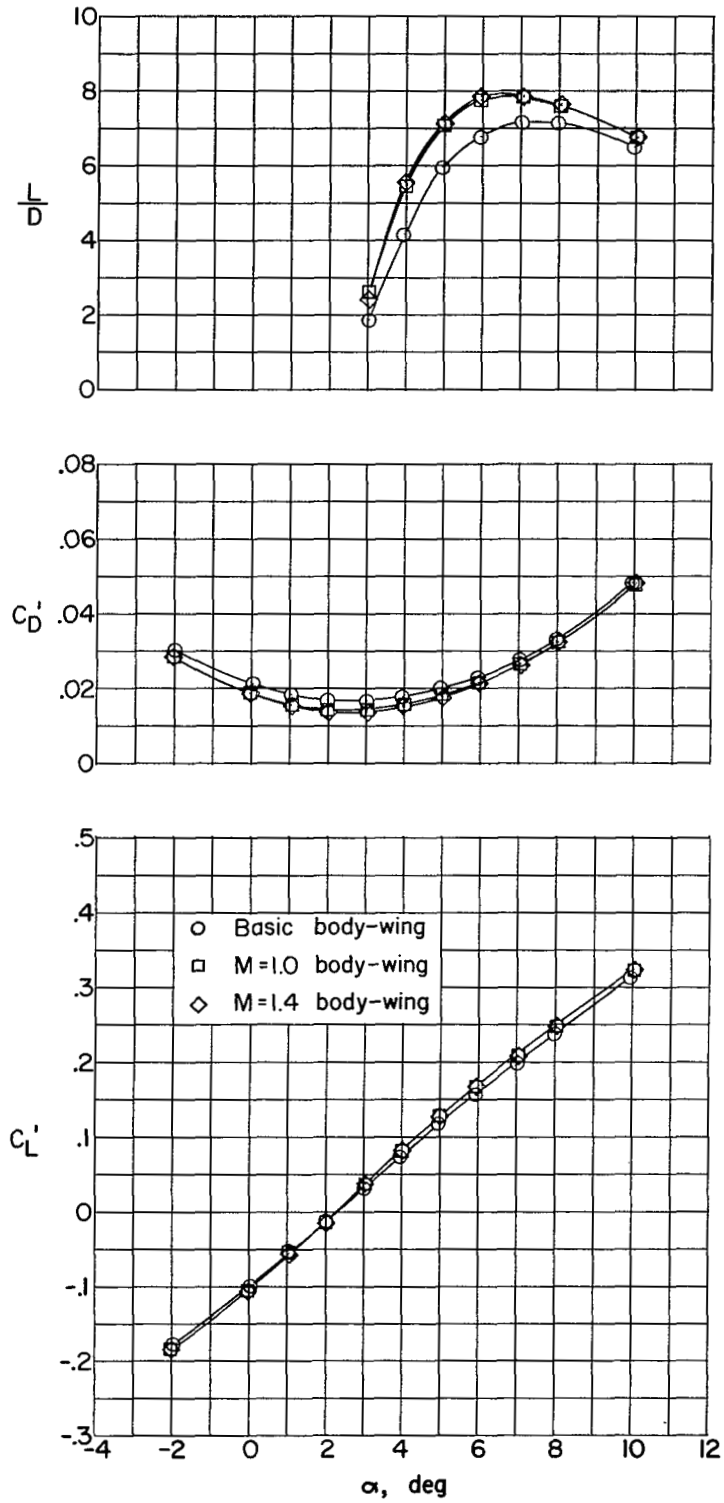

Figure 14.- Lift and drag characteristics of the three bodies in combination with the extended-chord wing at a Mach number of 1.61.

[redacted]

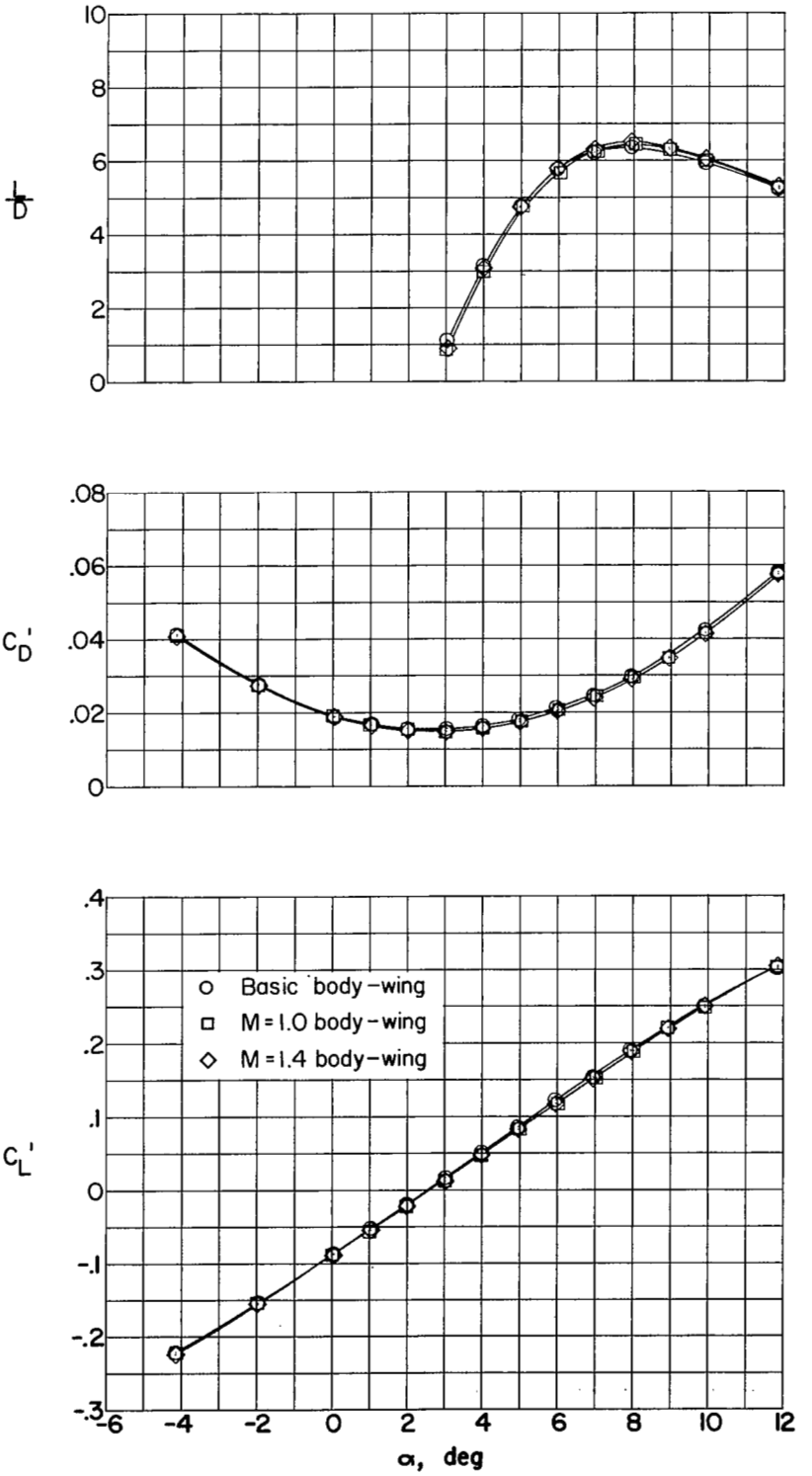

Figure 15.- Lift and drag characteristics of the three bodies in combination with the extended-chord wing at a Mach number of 2.01.

[redacted]

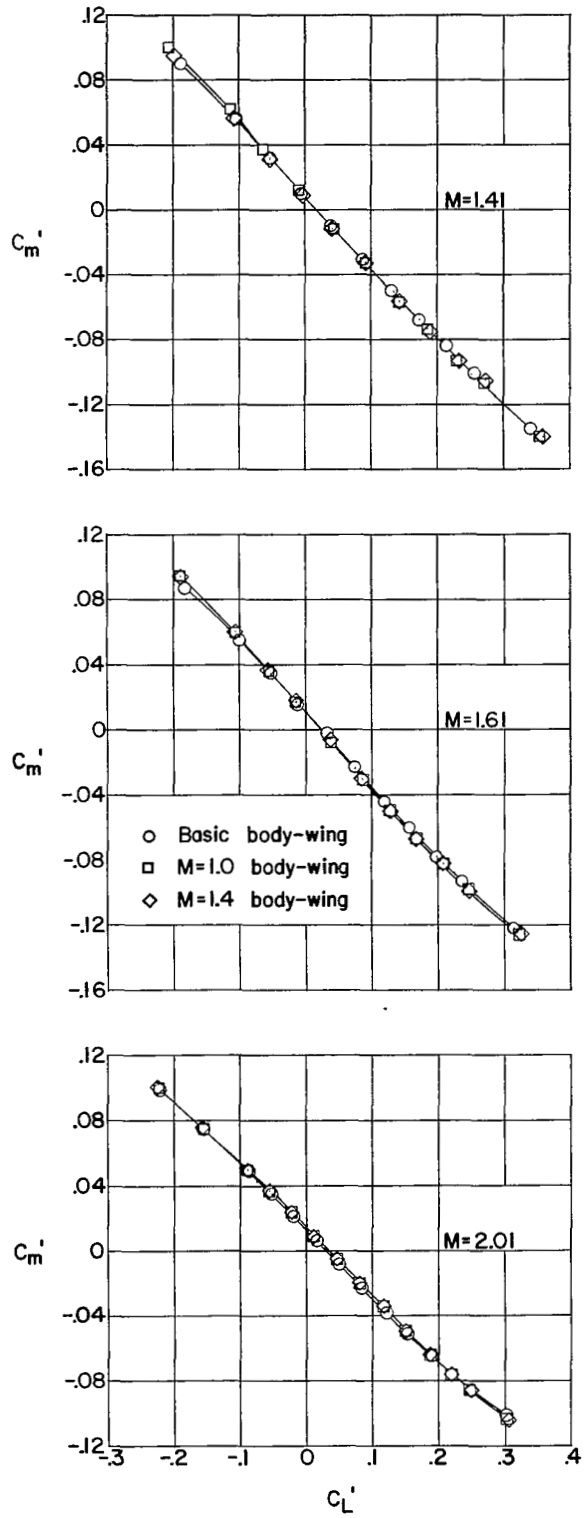

Figure 16.- Pitching-moment characteristics of the extended-chord wing-body configurations at Mach numbers of 1.41, 1.61, and 2.01.

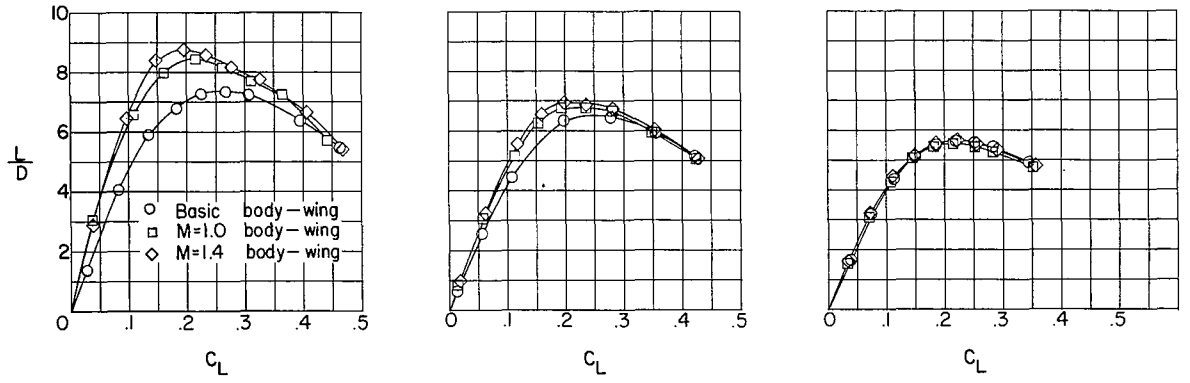

(a) 60° swept-wing—body configurations.

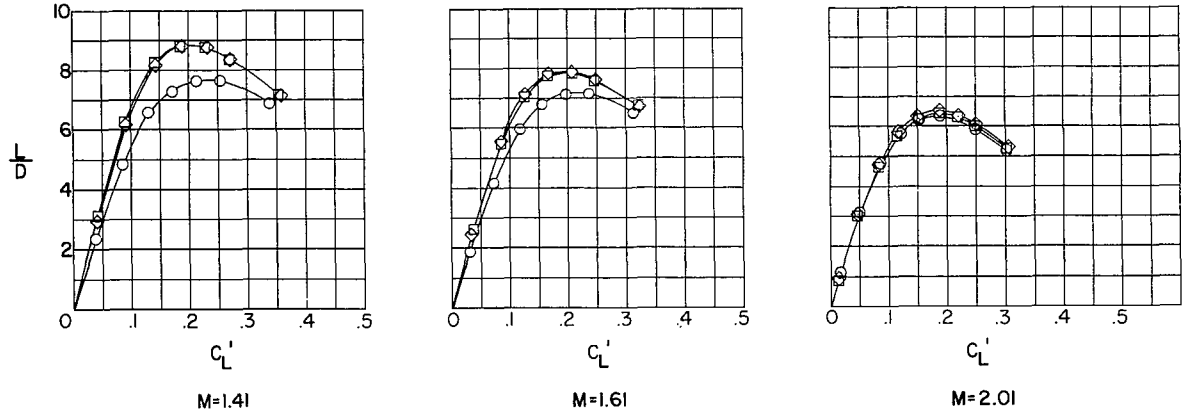

(b) Extended-chord wing-body configurations.

Figure 17.- Lift-drag ratio as a function of lift coefficient for the various configurations tested.

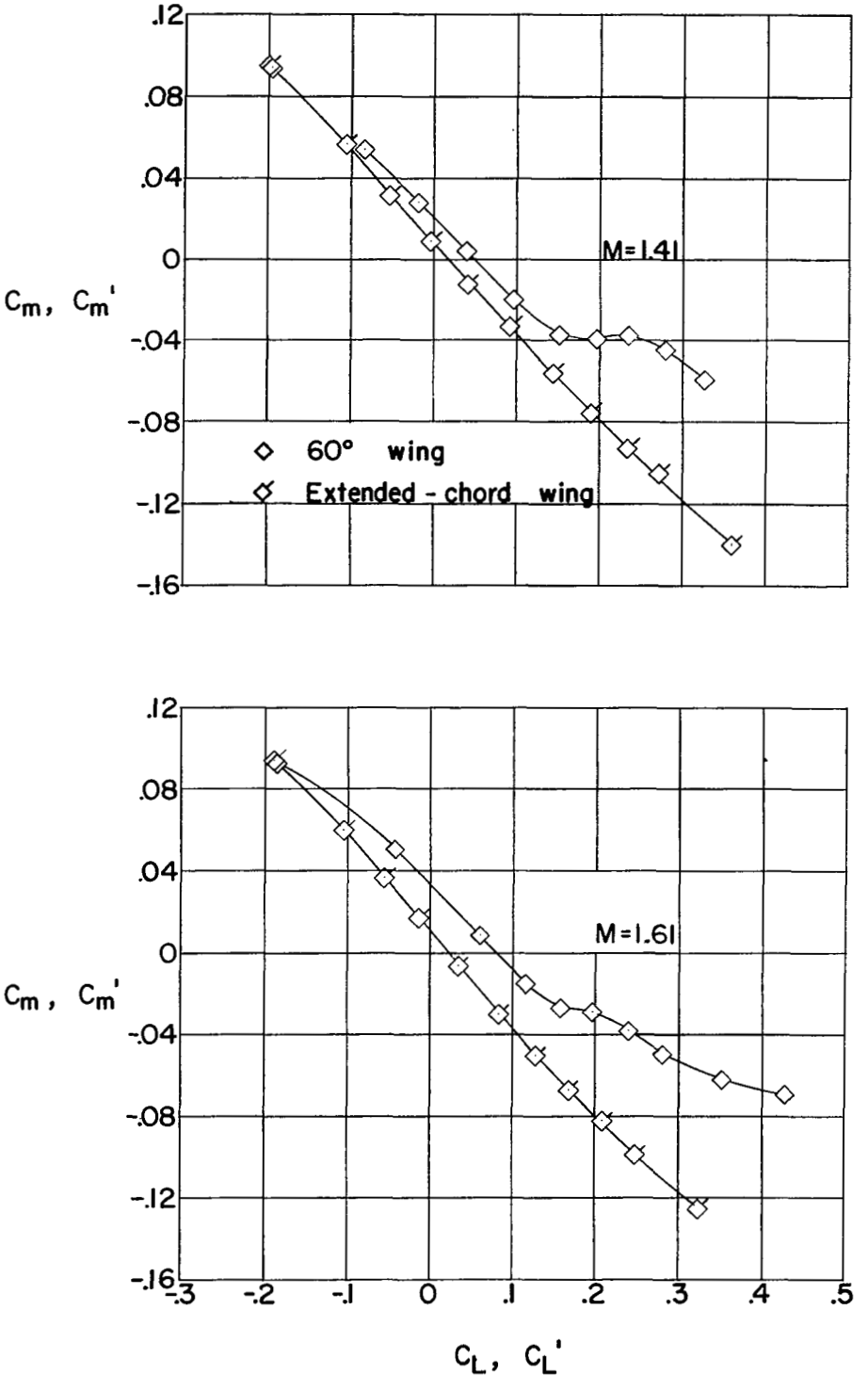

Figure 18.- Comparison of the pitching-moment characteristics of the 60° swept wing and the extended-chord wing (each in combination with the M = 1.4 body) at Mach numbers of 1.41 and 1.61.

[redacted]

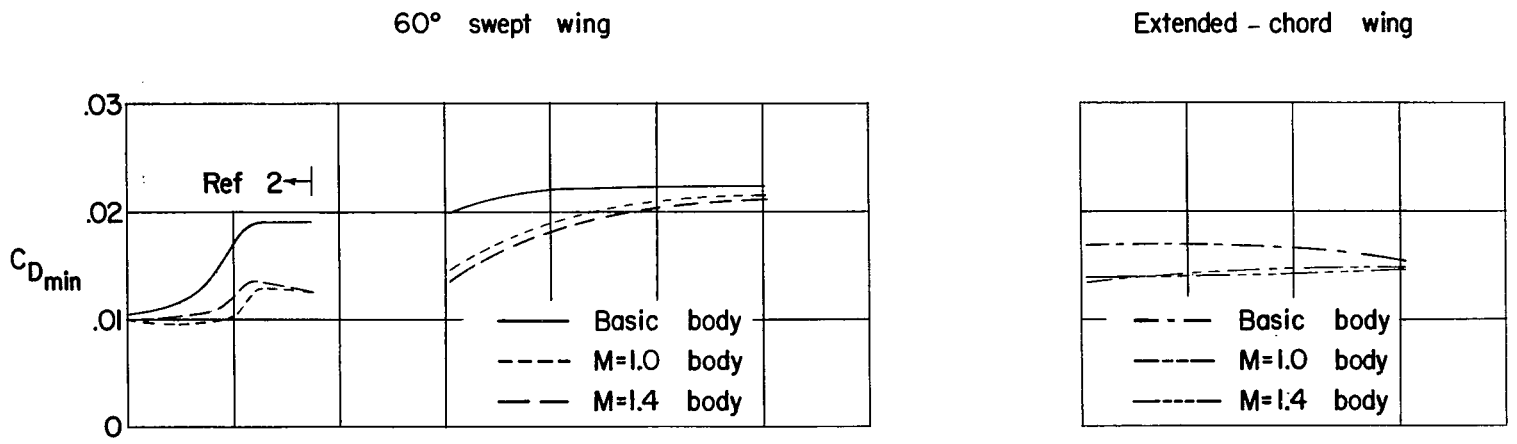

(a) Coefficients based on individual wing areas.

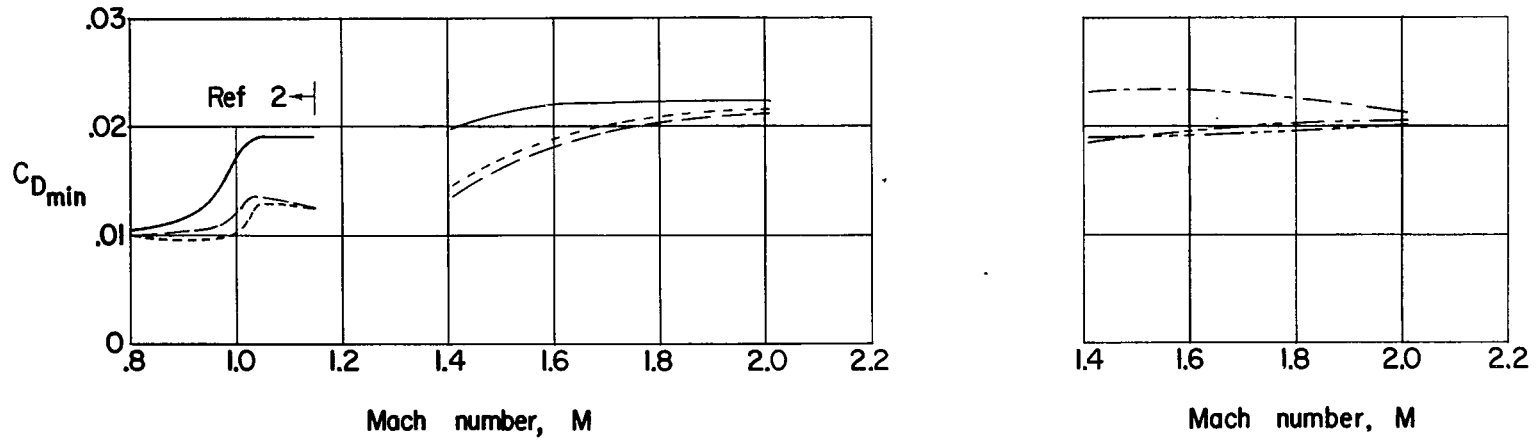

(b) Coefficients based on area of 60° swept wing.

Figure 19.- Variation of minimum drag coefficient with Mach number for the wing-body combinations tested.

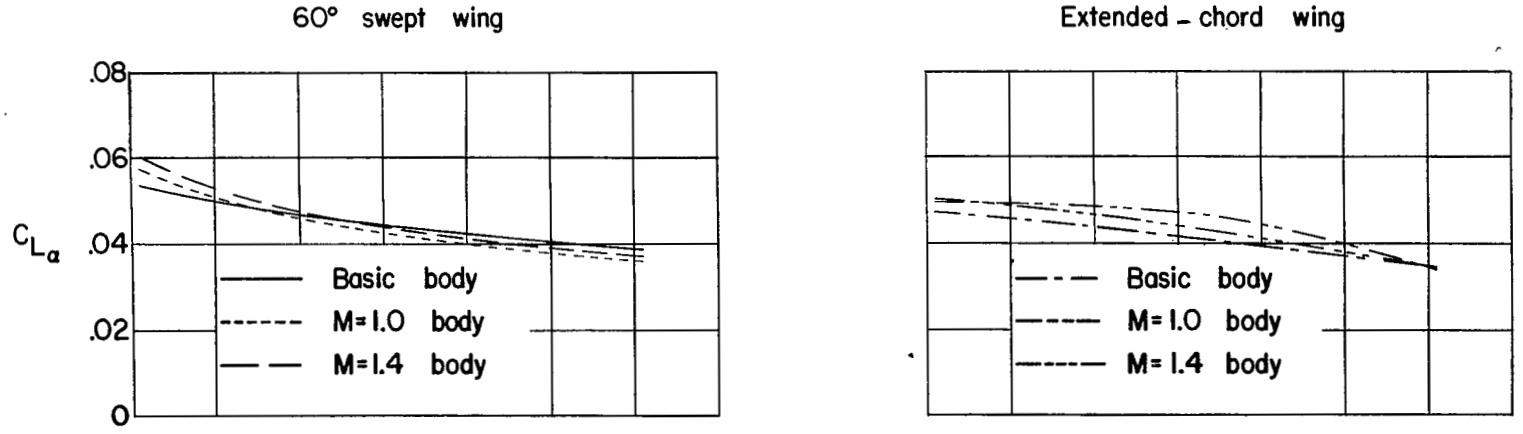

(a) Coefficients based on individual wing areas.

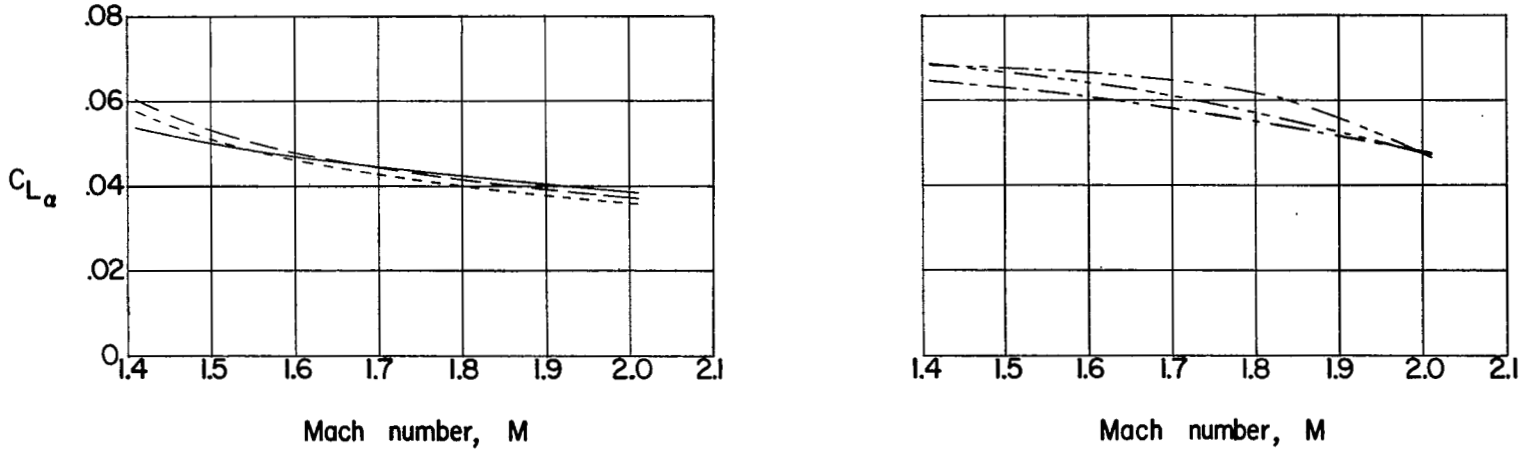

(b) Coefficients based on area of 60° swept wing.

Figure 20.- Variation with Mach number of lift-curve slope for the wing-body configurations tested.

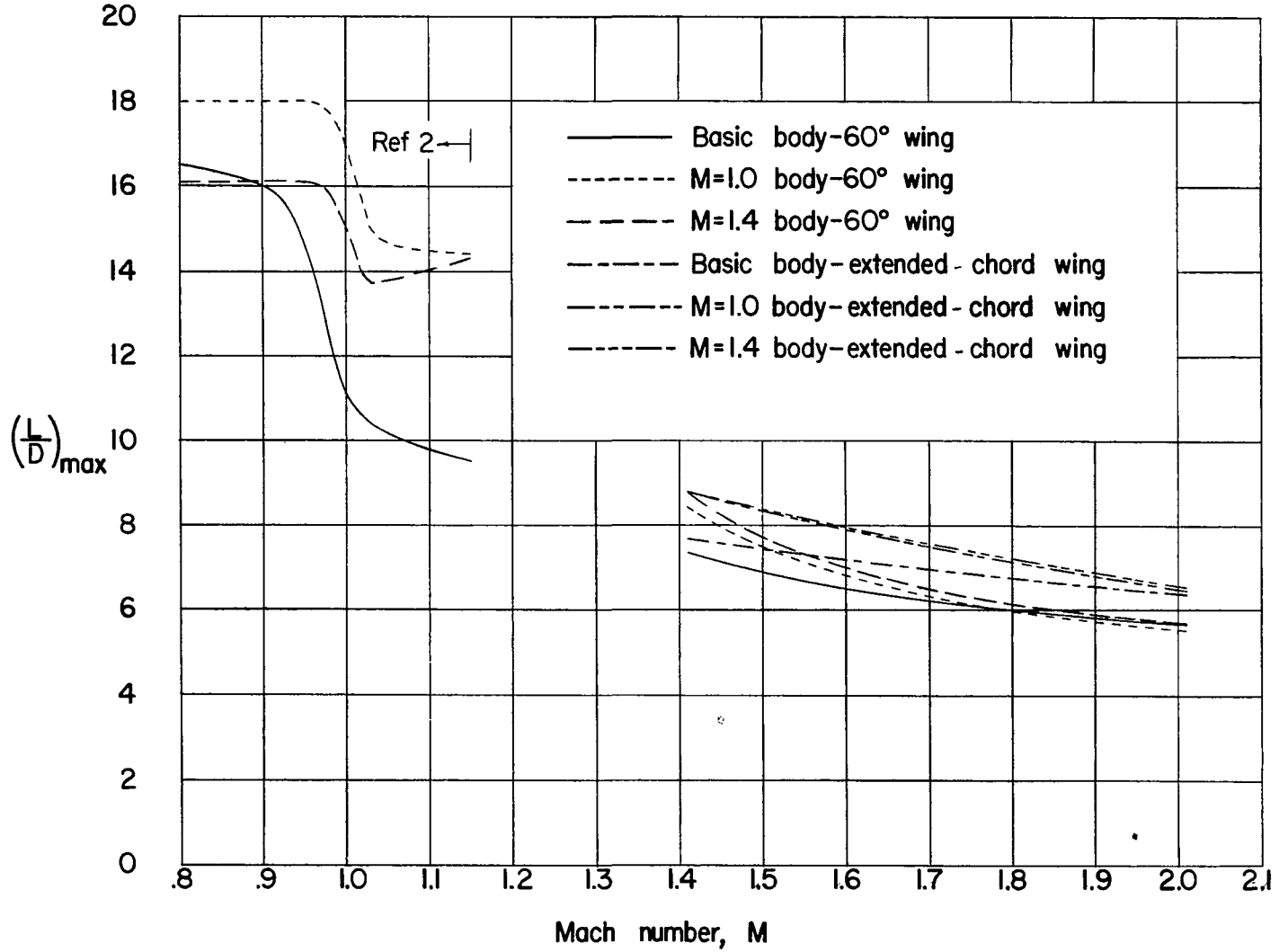

Figure 21.- Summary plot of maximum lift-drag ratio as a function of Mach number for all configurations tested.

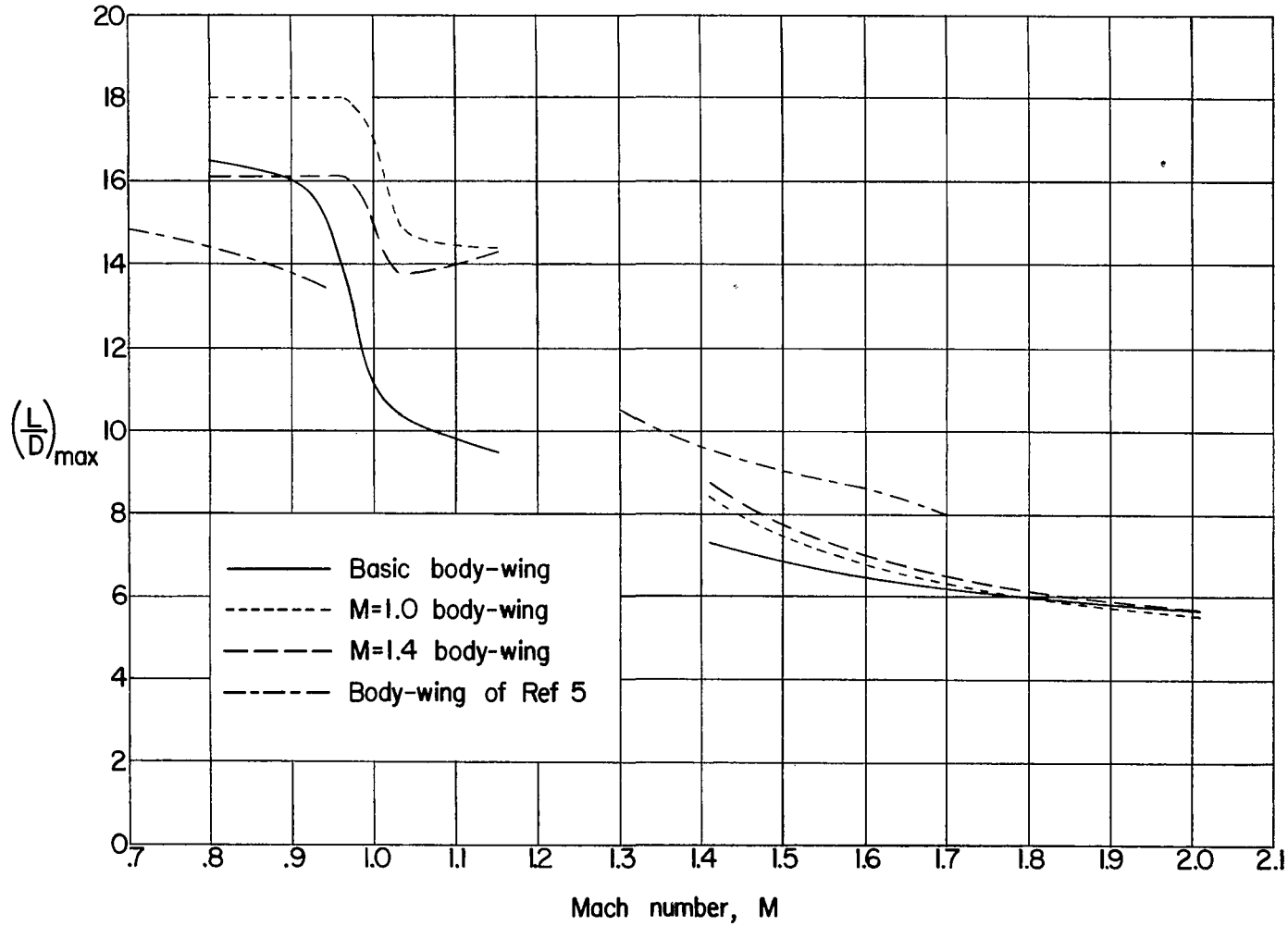

Figure 22.- Comparison of the 60° swept-wing—body configurations of this report with a configuration of similar plan form reported in reference 5.

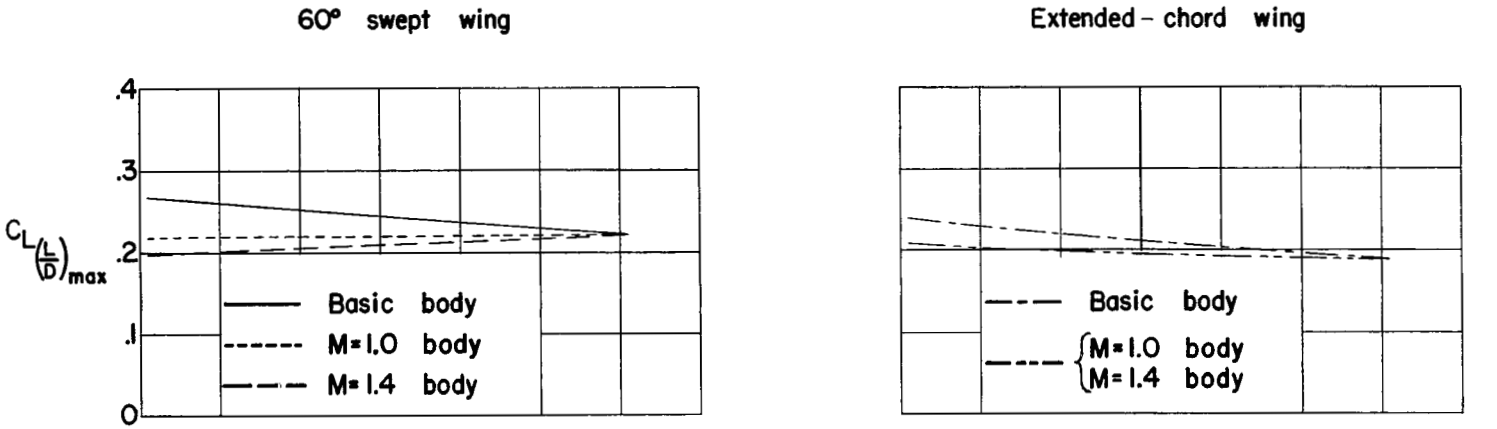

(a) Coefficients based on individual wing areas.

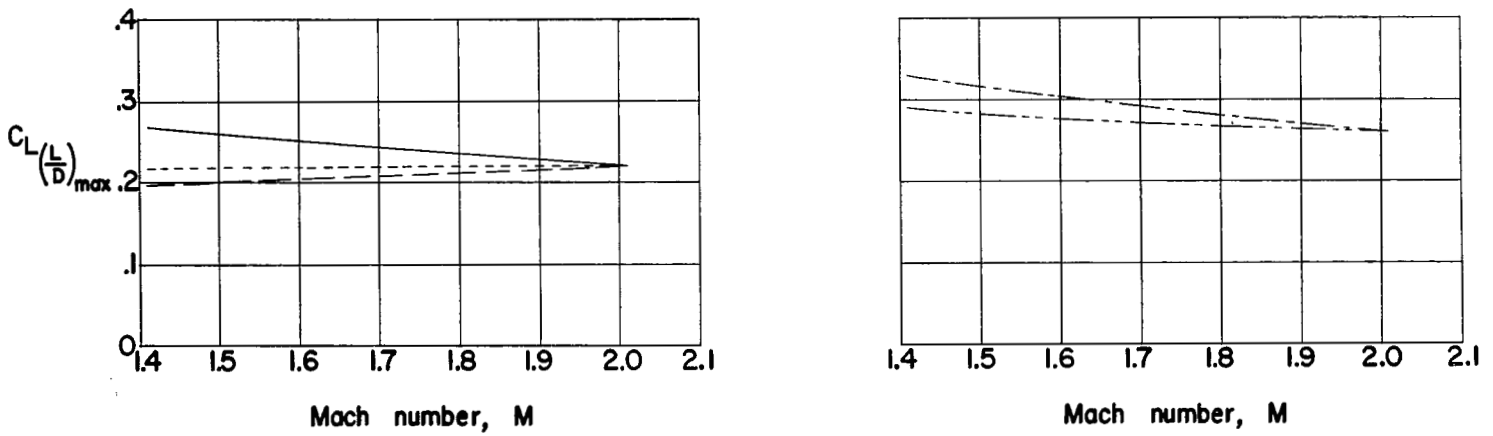

(b) Coefficients based on area of 60° swept wing.

Figure 23.- Variation with Mach number of the lift coefficient at which maximum lift-drag ratio occurs for the wing-body configurations tested.